



李政道研究所
Tsung-Dao Lee Institute



Recent Dark Matter combination summary from ATLAS

[arXiv:2306.00641](https://arxiv.org/abs/2306.00641)

The 4th Workshop on Frontiers of Particle Physics

Khanh N. Vu, Shu Li
on behalf of TDLI ATLAS group

August 08th, 2023

Outline

I. Recent ATLAS Dark Matter searches with 2HDM+a

1. Introduction on 2HDM+a
2. Experimental signatures
3. Statistical combination of results
4. Summary of constraints on 2HDM+a

II. Recent ATLAS $H \rightarrow \gamma\gamma_d$ searches in resonant $\gamma + E_T^{\text{miss}}$ signature

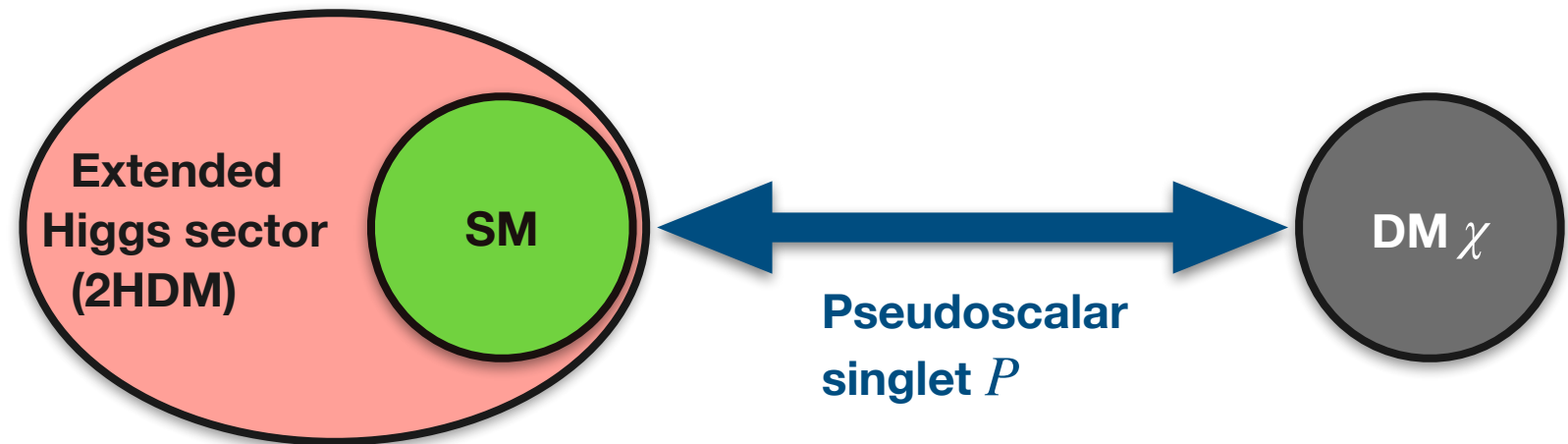
1. Results in VBF and ZH Higgs production modes
2. Prospects for statistical combination

I. Recent ATLAS Dark Matter searches with 2HDM+a

2HDM+a

• In this talk, ATLAS DM searches interpreted in **Two-Higgs-Doublet Model plus a pseudo-scalar mediator (2HDM+a)**:

- Minimal, UV-complete extension.
- EWK Symmetry Breaking:
 - 5 Higgs: h, H, H^\pm, A
 - 1 light pseudo-scalar: a



2HDM+a fully defined by 14 parameters

$v, M_h, M_A, M_H, M_{H^\pm}, M_a, m_\chi$
 $\cos(\beta - \alpha), \tan \beta, \sin \theta,$
 $y_\chi, \lambda_3, \lambda_{P1}, \lambda_{P2}$



EWK, flavour constraints and to simplify parameter space

5 unconstrained parameters

$m_A = m_H = m_{H^\pm}$
 m_a
 m_χ
 $\sin \theta$
 $\tan \beta$

masses of heavy Higgs

mass of pseudo-scalar mediator

DM mass

mixing angle between CP-odd states a and A

ratio of 2 Higgs doublet VEVs

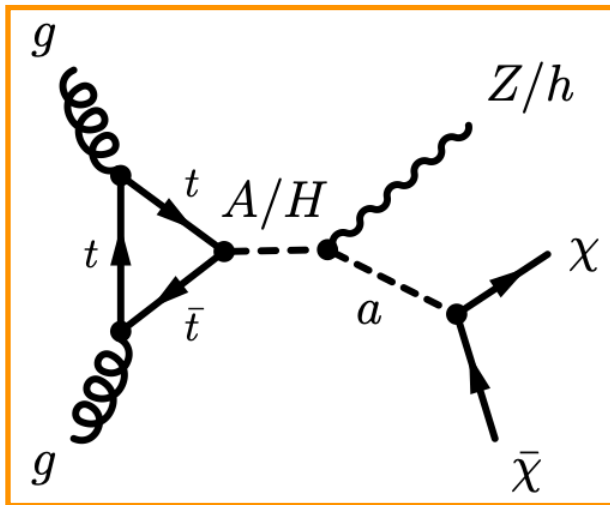
LHC Dark Matter Working Group
[Phys. Dark Univ. 27 \(2020\) 100351](#)
 Bauer, Haisch, Kahlhoefer
[JHEP05\(2017\) 138](#)

* h : SM-like CP-even Higgs with mass of 125 GeV

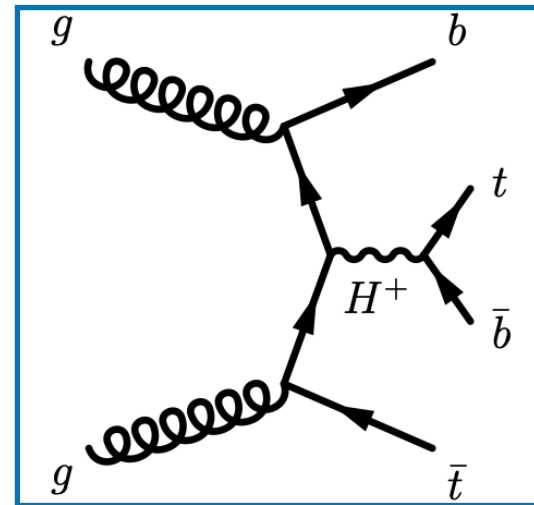
Experimental signatures

• 2HDM+a has rich phenomenology predicting wide range of signatures with both visible and invisible decays

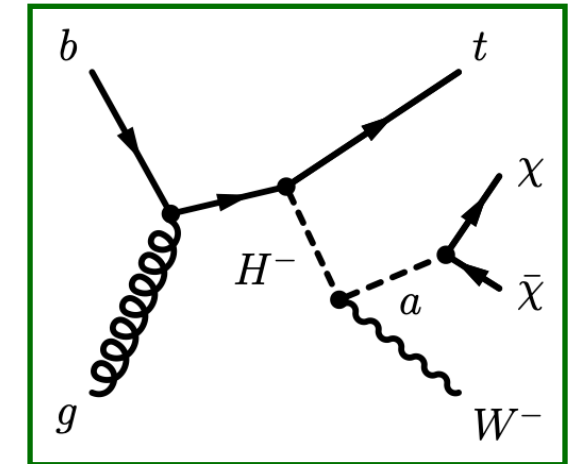
- ▶ resonantly production of $E_T^{\text{miss}} + Z/h$ (mono- Z/h)
- ▶ additional (pseudo-)scalar bosons, e.g. $tbH^\pm(tb)$
- ▶ new signatures, e.g. $E_T^{\text{miss}} + tW$ (backup slides)



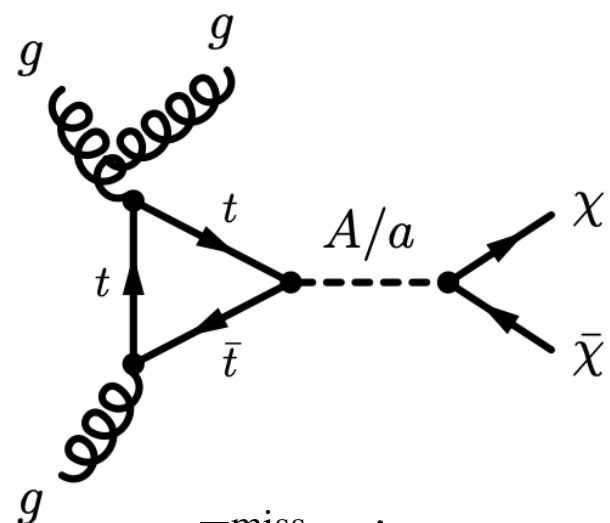
$E_T^{\text{miss}} + Z/h$



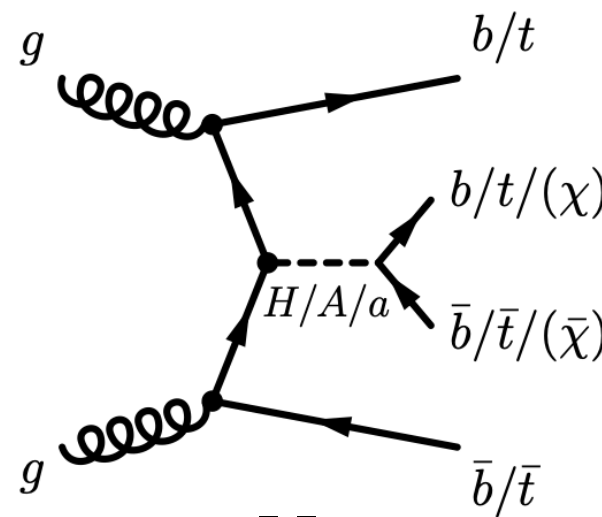
$tbH^\pm(tb)$



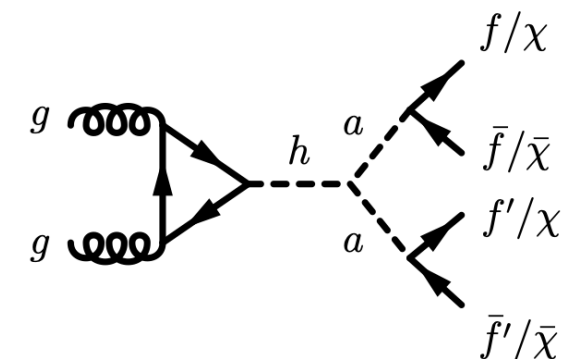
$E_T^{\text{miss}} + tW$



$E_T^{\text{miss}} + \text{jet}$



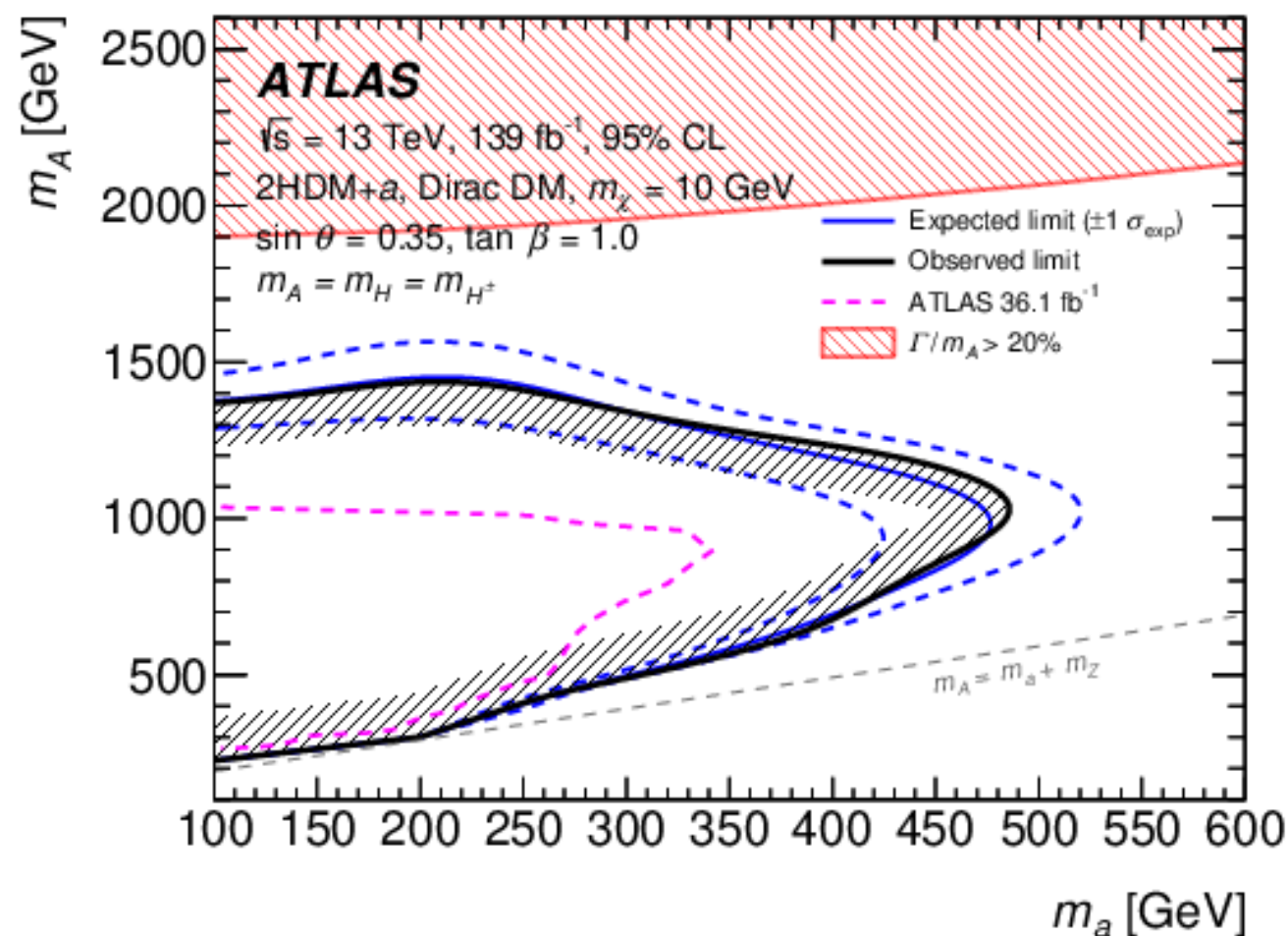
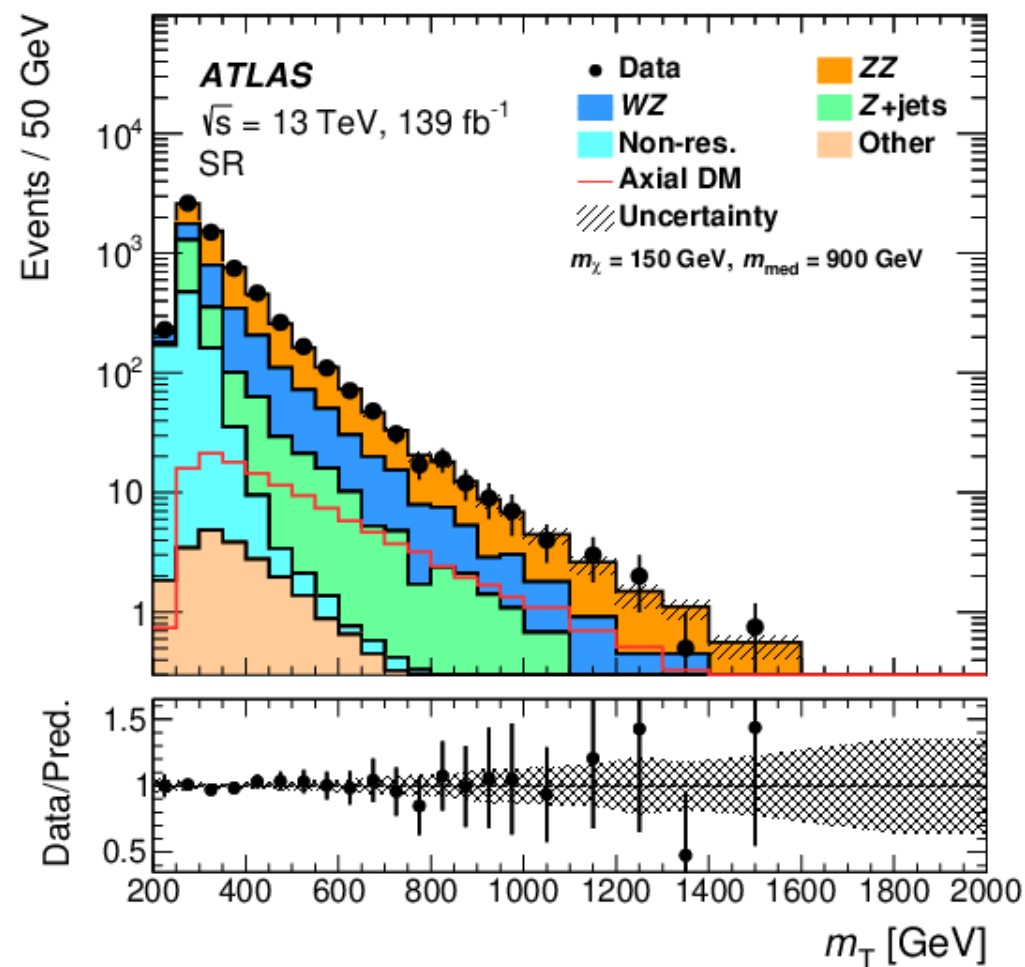
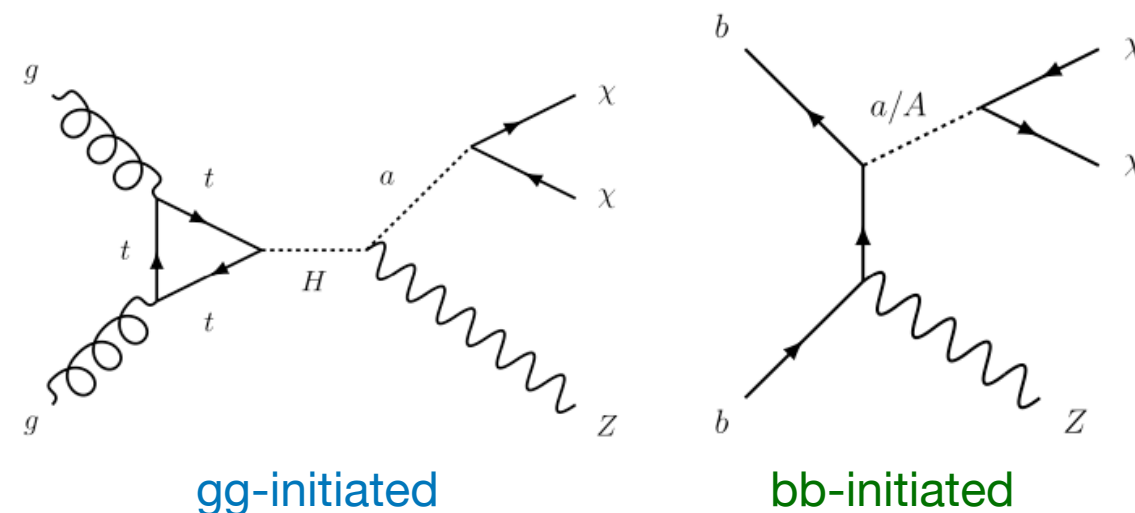
$t\bar{t}t\bar{t}$



$h \rightarrow aa \rightarrow 4f/h \rightarrow \text{invisible}$

$E_T^{\text{miss}} + Z(ll)$ signature

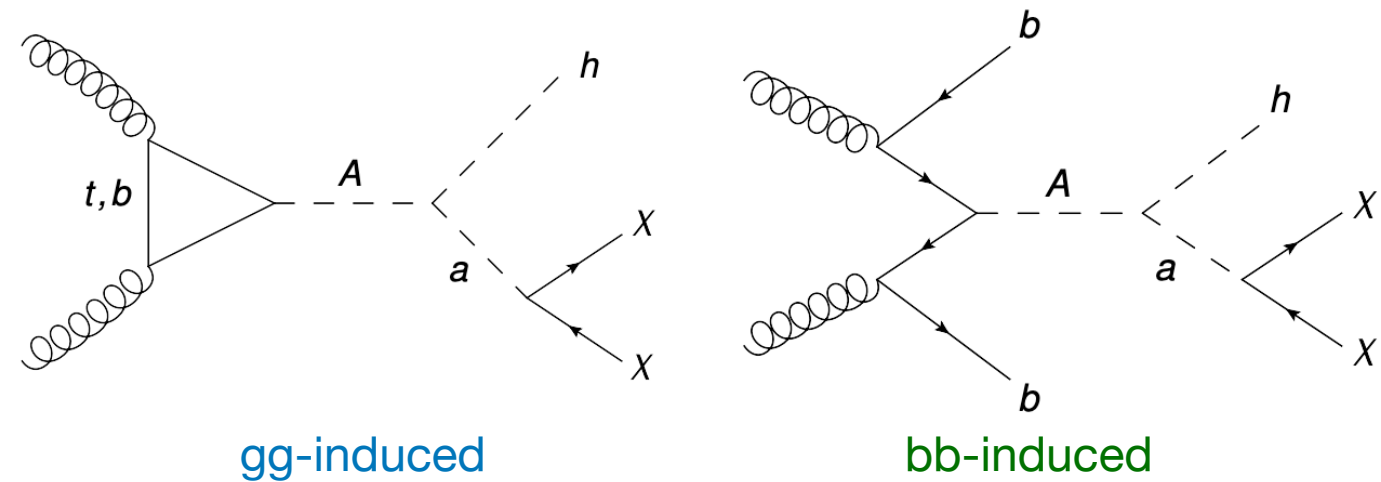
- Z boson recoiling against large E_T^{miss}
 - $E_T^{\text{miss}} > 90$ GeV
- Presence of a pair of high- p_T , same flavour, oppositely charged leptons with angular separation < 1.8
- Fit to data is performed on
 - m_T^{lep} in signal region and region constraining non-resonant backgrounds.
 - E_T^{miss} in regions constraining di-boson backgrounds



$$m_T^{\text{lep}} = \sqrt{\left[\sqrt{m_Z^2 + (p_T^{\ell\ell})^2} + \sqrt{m_Z^2 + (E_T^{\text{miss}})^2} \right]^2 - \left[\vec{p}_T^{\ell\ell} + \vec{p}_T^{\text{miss}} \right]^2}$$

$E_T^{\text{miss}} + h(bb)$ signature

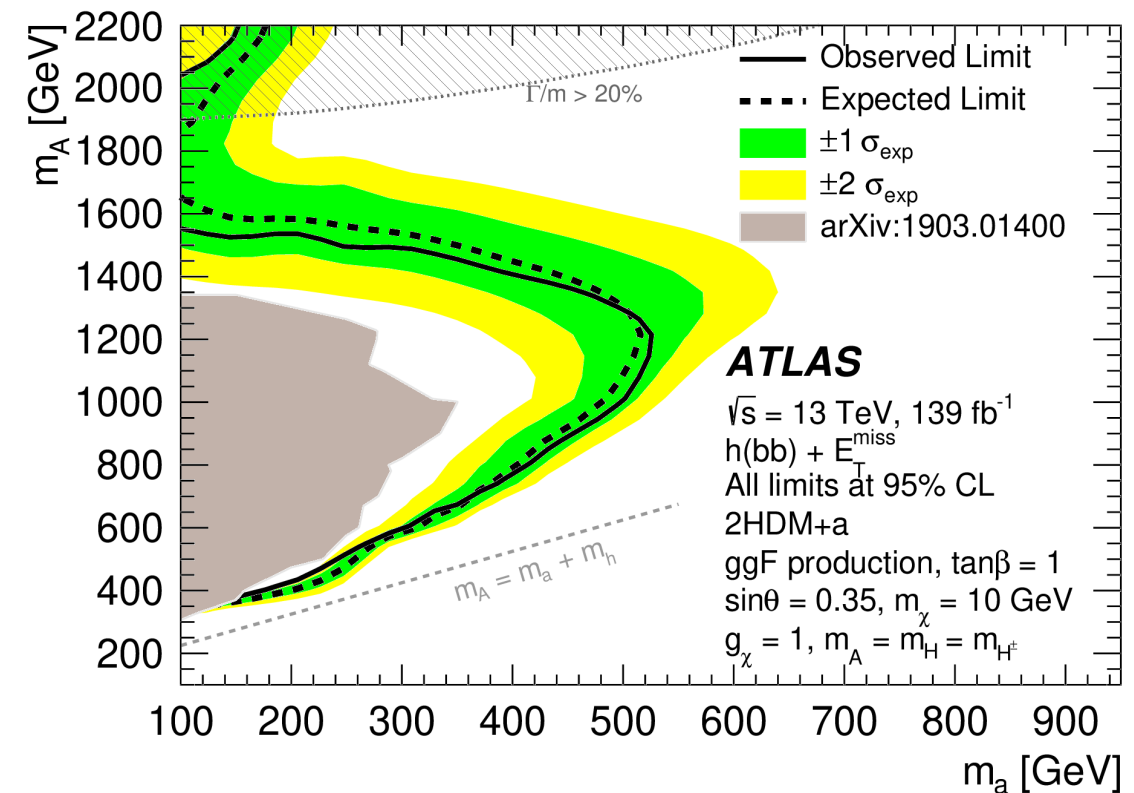
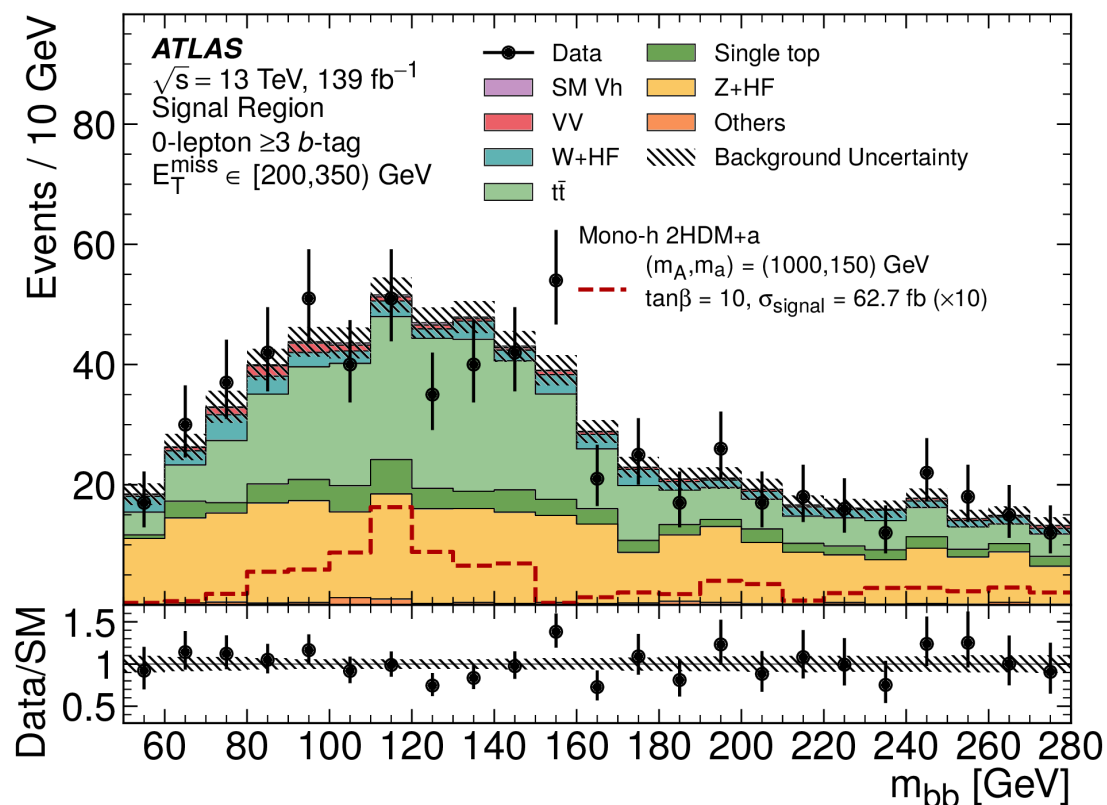
- Higgs boson recoiling against large E_T^{miss}
 - $E_T^{\text{miss}} > 150$ GeV
- targets both **gg-induced** and **bb-induced** production
 - 2 categories: ≥ 2 b-jets or ≥ 3 b-jets.



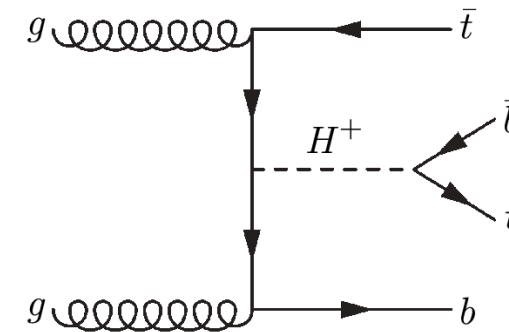
- each category split into orthogonal E_T^{miss} bins
 - Higgs decay reconstructed as single large-R jet for $E_T^{\text{miss}} > 500$ GeV



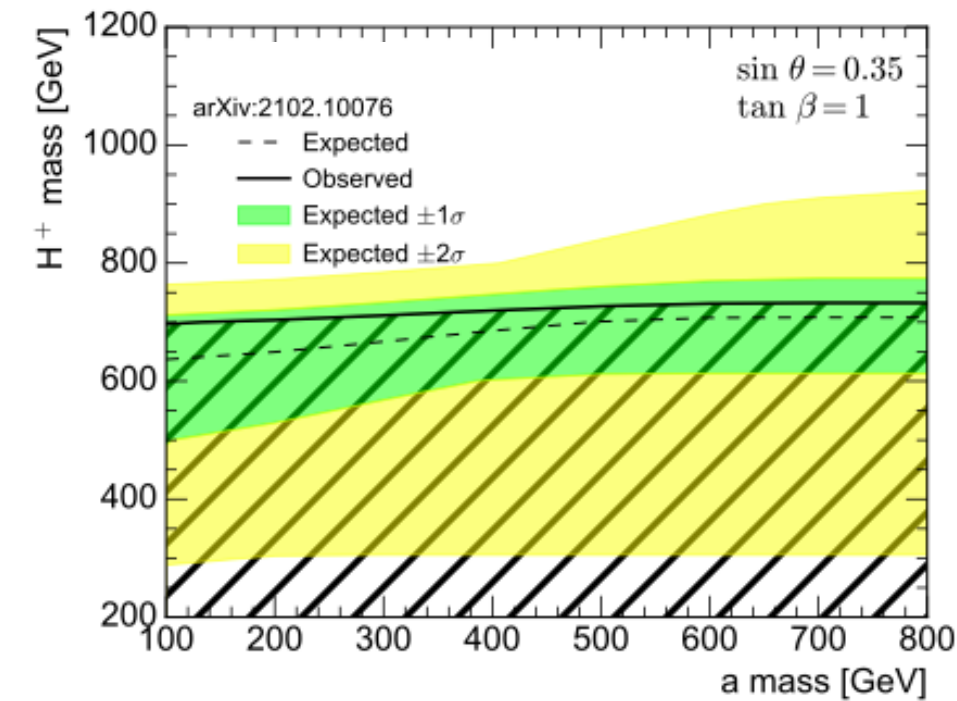
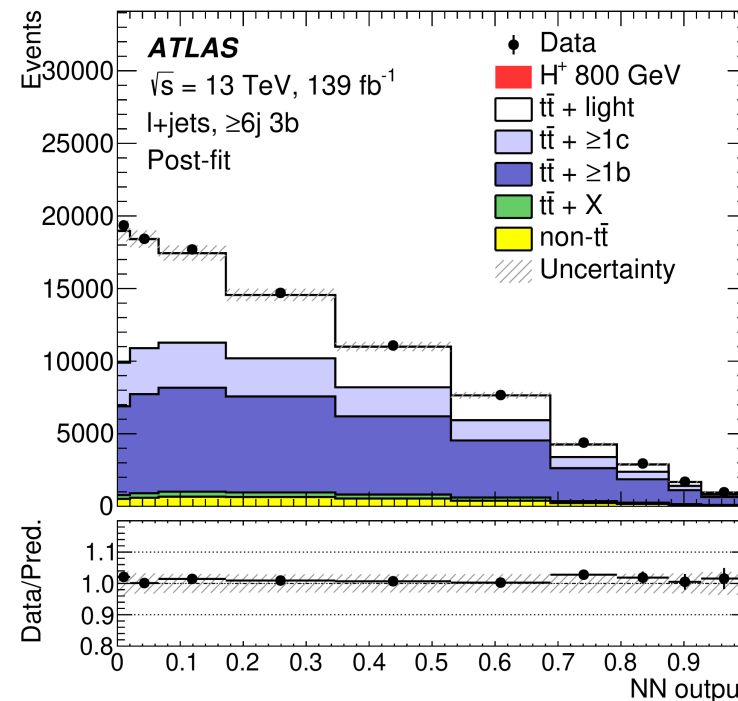
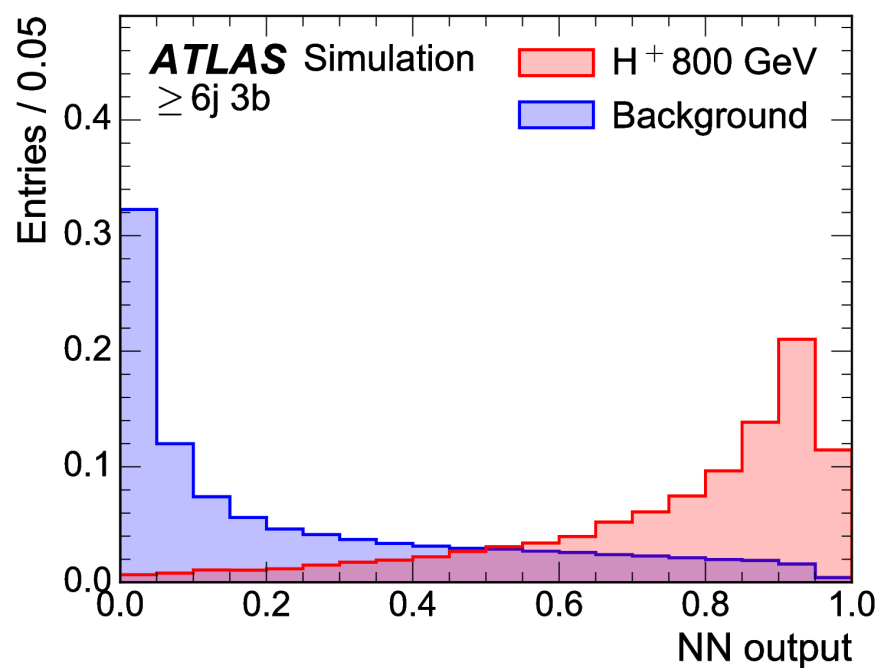
- Fit to data: m_{bb} (in signal regions) + event yields (in background-constrained regions).



$tbH^\pm(tb)$ signature

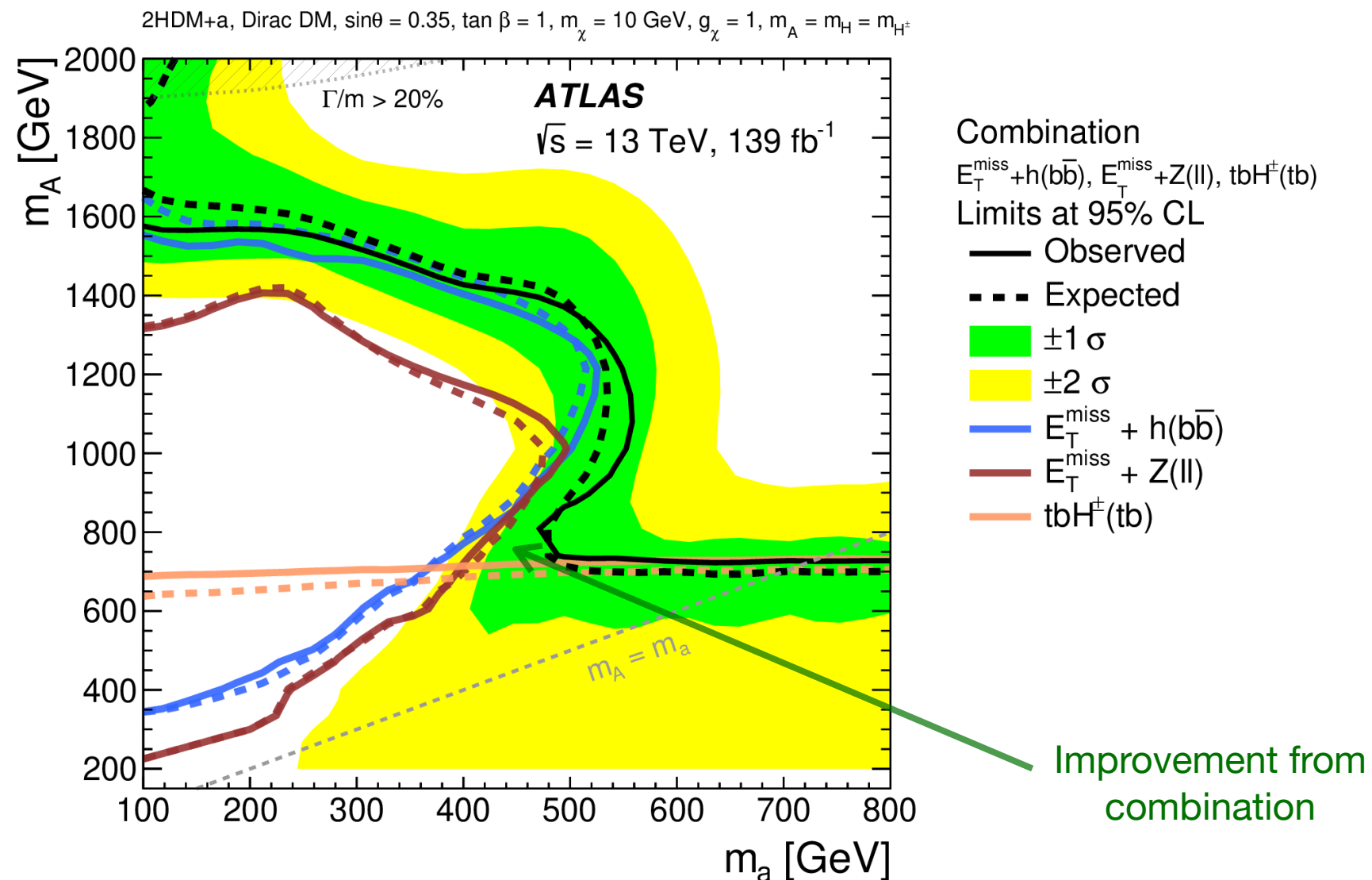


- original analysis for 2HDM type-II, searching heavy charged Higgs, mass in [0.2, 2] TeV.
 - re-interpreted for 2HDM+a by rescaling 2HDM type-II exclusion limits.
- targets semileptonic decay of one of top quarks
 - 1 lepton, ≥ 5 jets, ≥ 3 b-jets.
- 4 separate signal regions according to jet and b-jet multiplicity.
- Fit to data performed on a Neural Network distribution across regions.



Statistical combination

- $E_T^{\text{miss}} + h(bb)$, $E_T^{\text{miss}} + Z(ll)$ and $tbH^\pm(tb)$: Most constraining signatures of 2HDM+a.
 - $tbH^\pm(tb)$ gives significant complementarity to sensitivities of $E_T^{\text{miss}} + X$
 - stat. combination of 3 channels to maximize 2HDM+a constraints in parameter space.
- Combined exclusion limits obtained from **profile likelihood ratio** corresponding to **3-channel-combined likelihood**.
- Decorrelate over-constrained/pulled uncertainties to avoid any phase-space-specific biases across channels.



Summary of constraints on 2HDM+a

- constraints on 2HDM+a interpreted in **6 benchmark scenarios**.
 - highlight diverse phenomenology of 2HDM+a.
 - study the interplay and complementarities between different signatures.

Scenario		Fixed parameter values				Varied parameters
		$\sin \theta$	m_A [GeV]	m_a [GeV]	$\tan \beta$	
1	a	0.35	–	–	1.0	(m_a, m_A)
	b	0.70	–	–	1.0	
2	a	0.35	–	250	–	$(m_A, \tan \beta)$
	b	0.70	–	250	–	
3	a	0.35	600	–	–	$(m_a, \tan \beta)$
	b	0.70	600	–	–	
4	a	–	600	200	1.0	$\sin \theta$
	b	–	1000	350	1.0	
5		0.35	1000	400	1.0	m_χ
6		0.35	1200	–	1.0	(m_a, m_χ)

shows interplay due to mass hierarchies

motivated by similar scans done for general 2HDMs

illustration a - A mixing parameter effect

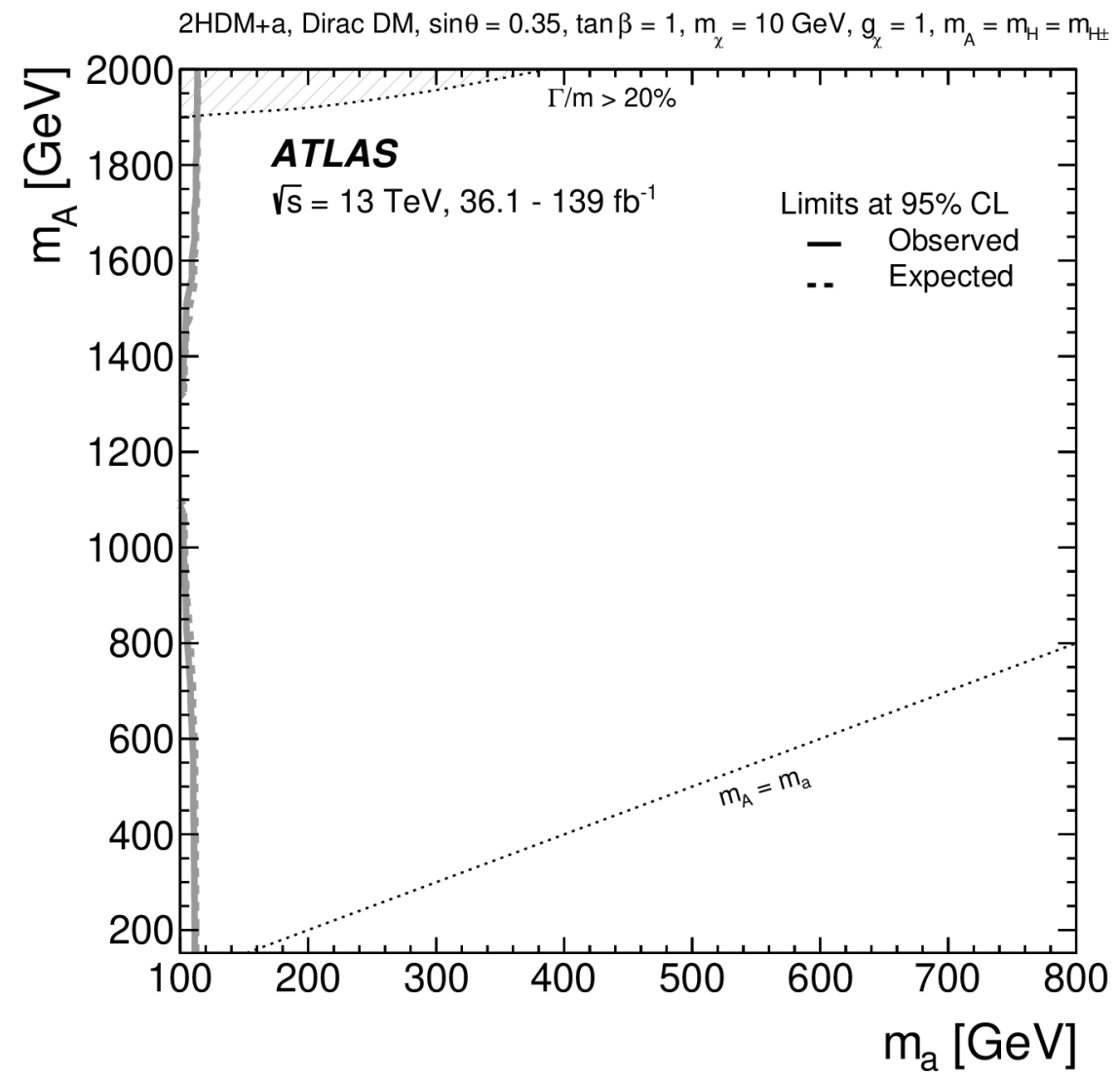
connection with cosmological constraints and direct/indirect searches

showed for the 1st time

m_χ set to 10 GeV in all scenarios, except 5 and 6

Scenario 1a: $\sin \theta = 0.35$ m_A - m_a plane

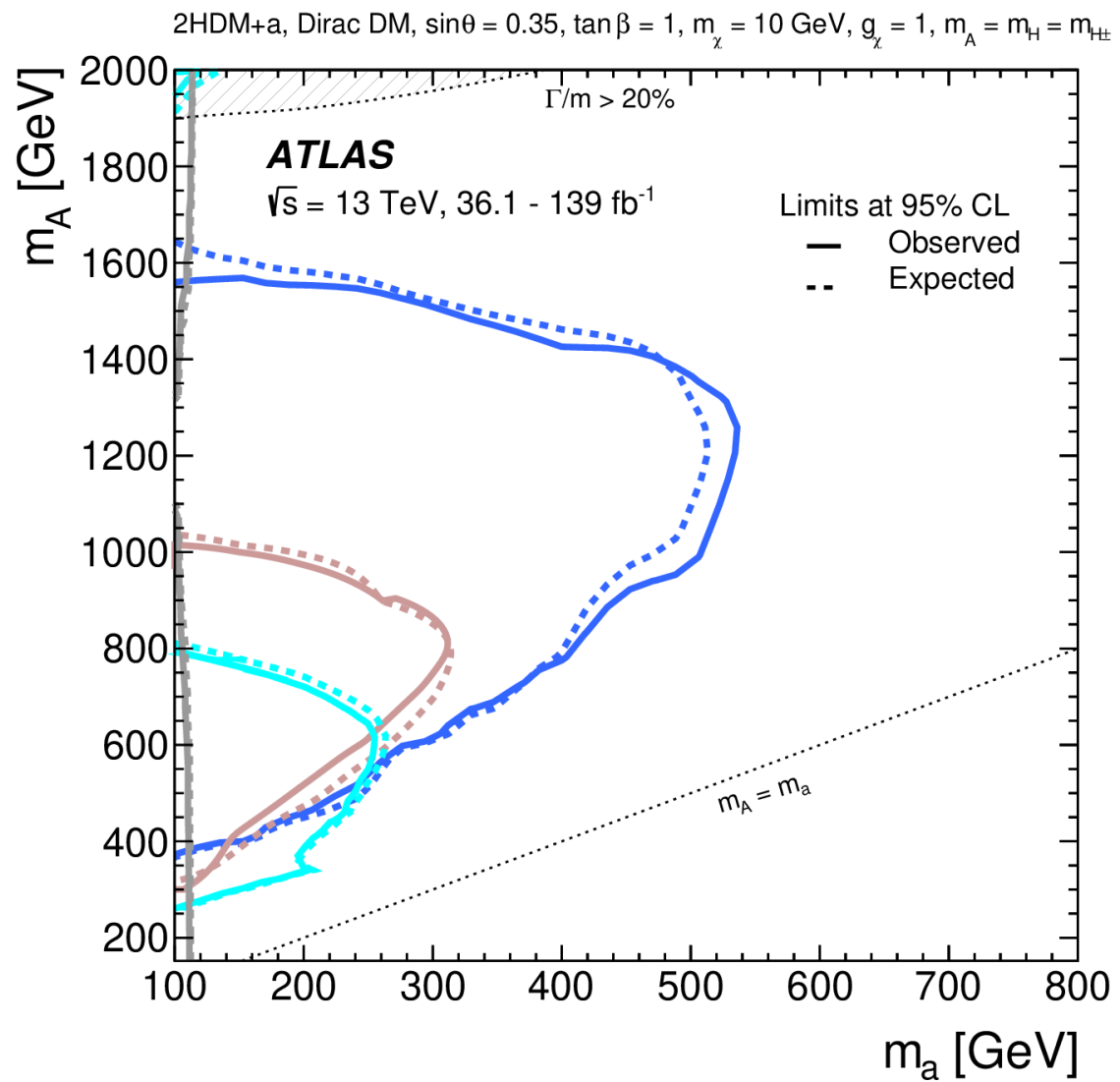
- $h \rightarrow$ invisible constrains very low m_a .



— $h \rightarrow$ invisible, 139 fb⁻¹
arxiv:2301.10731

Scenario 1a: $\sin \theta = 0.35$ m_A - m_a plane

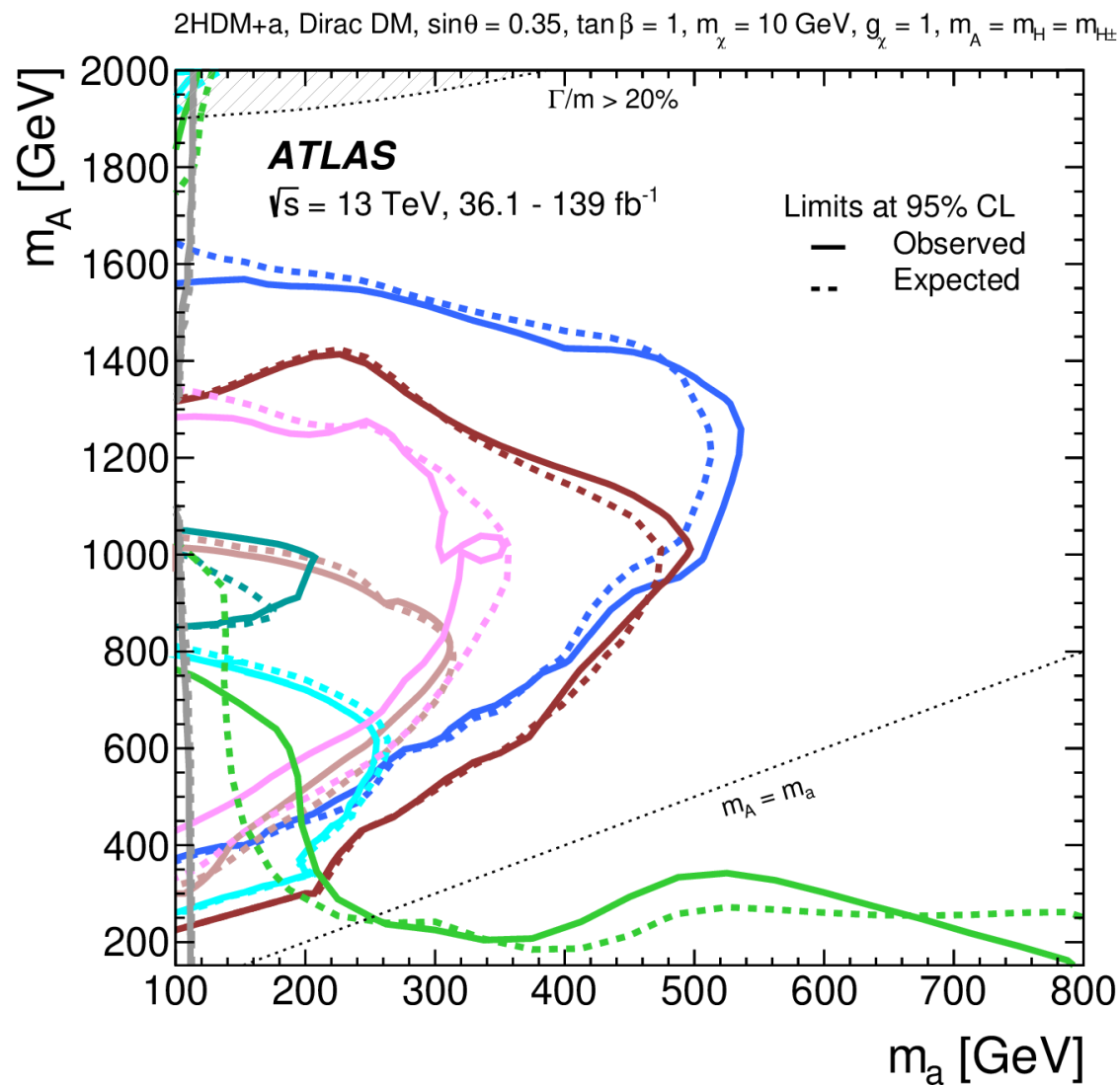
- $h \rightarrow$ invisible constrains very low m_a .
- constraints from $E_T^{\text{miss}} + h$ signatures: similar m_A - m_a dependence, with $h \rightarrow bb$ most sensitive.



- $E_T^{\text{miss}} + h(b\bar{b})$, 139 fb⁻¹
 JHEP 11 (2021) 209
- $E_T^{\text{miss}} + h(\tau\tau)$, 139 fb⁻¹
 arXiv:2305.12938
- $E_T^{\text{miss}} + h(\gamma\gamma)$, 139 fb⁻¹
 JHEP 10 (2021) 13
- $h \rightarrow$ invisible, 139 fb⁻¹
 arxiv:2301.10731

Scenario 1a: $\sin \theta = 0.35$ m_A - m_a plane

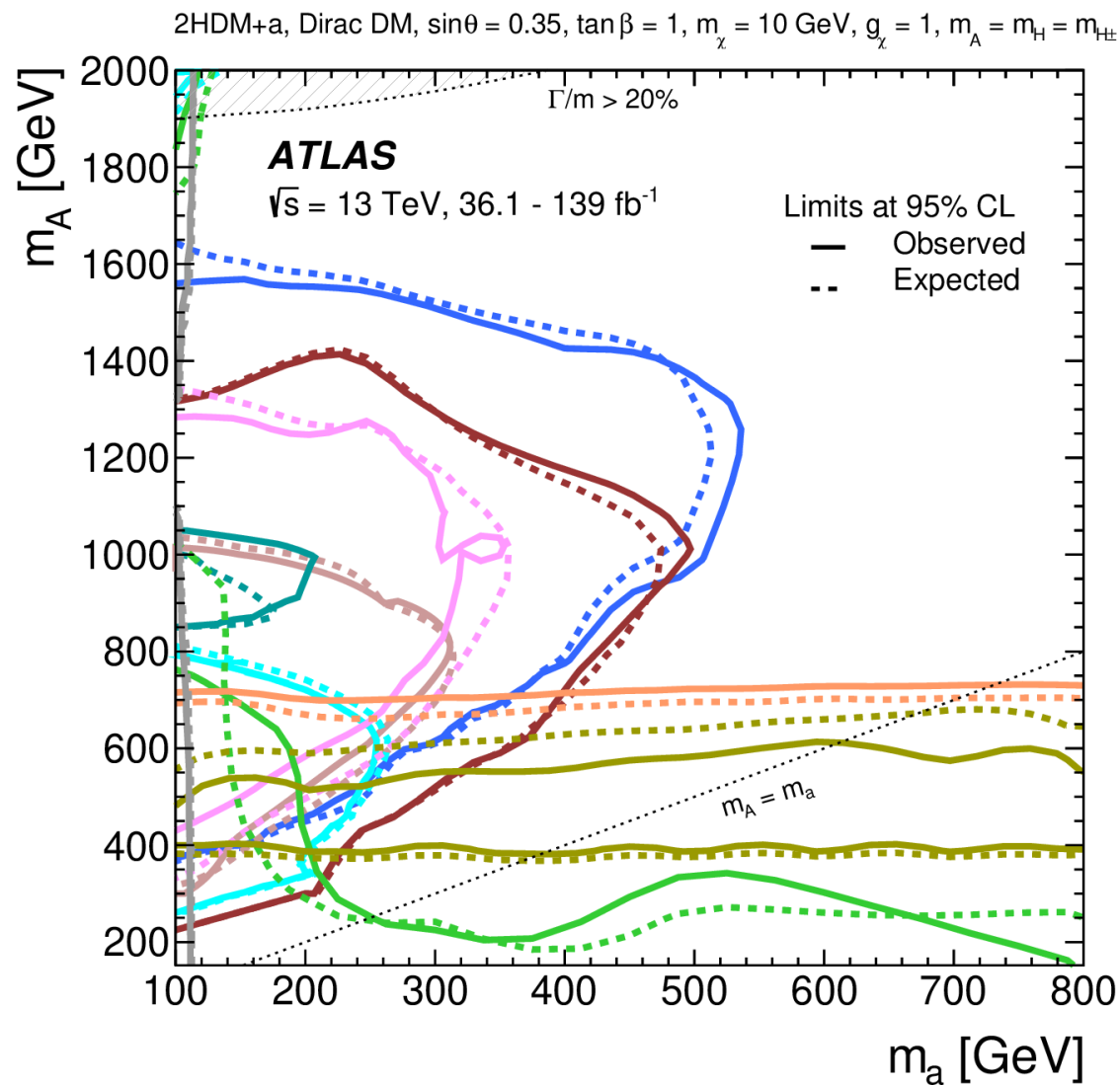
- $h \rightarrow$ invisible constrains very low m_a .
- constraints from $E_T^{\text{miss}} + h$ signatures: similar m_A - m_a dependence, with $h \rightarrow bb$ most sensitive.
- $E_T^{\text{miss}} + tW$ similar to $E_T^{\text{miss}} + Z(\ell\ell)$ but with smaller excl. region.
- $E_T^{\text{miss}} + \text{jet}$ sensitivity notably different from those of $E_T^{\text{miss}} + Z$ and $E_T^{\text{miss}} + h$.



- $E_T^{\text{miss}} + h(b\bar{b})$, 139 fb⁻¹
 JHEP 11 (2021) 209
- $E_T^{\text{miss}} + h(\tau\tau)$, 139 fb⁻¹
 arXiv:2305.12938
- $E_T^{\text{miss}} + h(\gamma\gamma)$, 139 fb⁻¹
 JHEP 10 (2021) 13
- $E_T^{\text{miss}} + Z(\ell\ell)$, 139 fb⁻¹
 PLB 829 (2022) 137066
- $E_T^{\text{miss}} + Z(q\bar{q})$, 36.1 fb⁻¹
 JHEP 10 (2018) 180
- $E_T^{\text{miss}} + tW$, 139 fb⁻¹
 arXiv:2211.13138
- $E_T^{\text{miss}} + j$, 139 fb⁻¹
 PRD 103 (2021) 112006
- $h \rightarrow$ invisible, 139 fb⁻¹
 arxiv:2301.10731

Scenario 1a: $\sin \theta = 0.35$ m_A - m_a plane

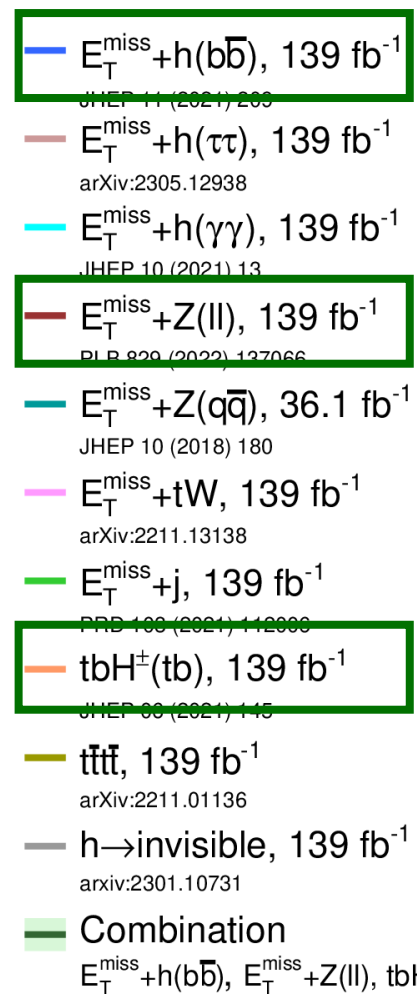
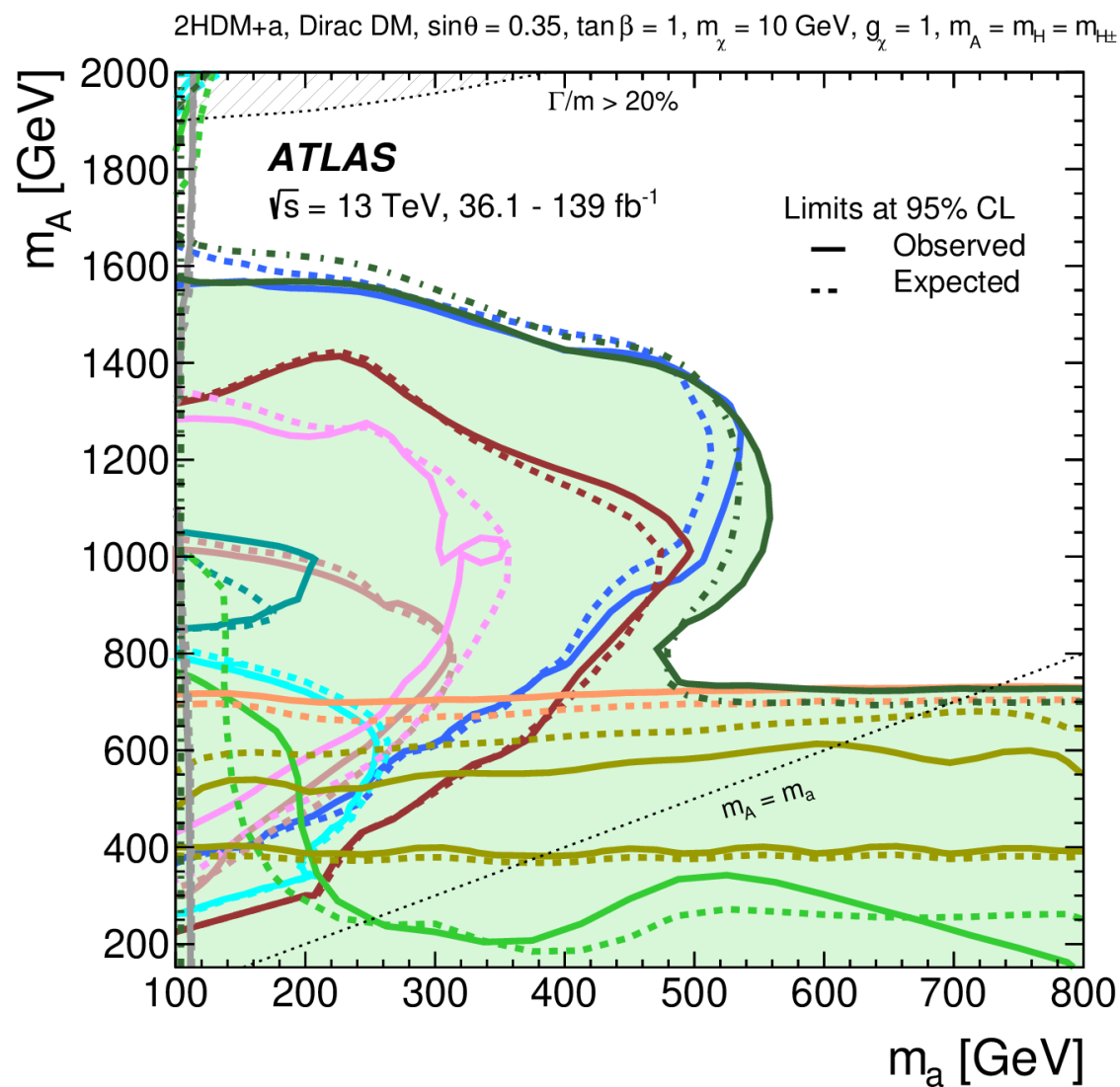
- $h \rightarrow$ invisible constrains very low m_a .
- constraints from $E_T^{\text{miss}} + h$ signatures: similar m_A - m_a dependence, with $h \rightarrow bb$ most sensitive.
- $E_T^{\text{miss}} + tW$ similar to $E_T^{\text{miss}} + Z(\ell\ell)$ but with smaller excl. region.
- $E_T^{\text{miss}} + \text{jet}$ sensitivity notably different from those of $E_T^{\text{miss}} + Z$ and $E_T^{\text{miss}} + h$.
- Complementary constraints from searches not targeting DM.



- $E_T^{\text{miss}} + h(b\bar{b})$, 139 fb⁻¹
 JHEP 11 (2021) 209
- $E_T^{\text{miss}} + h(\tau\tau)$, 139 fb⁻¹
 arXiv:2305.12938
- $E_T^{\text{miss}} + h(\gamma\gamma)$, 139 fb⁻¹
 JHEP 10 (2021) 13
- $E_T^{\text{miss}} + Z(\ell\ell)$, 139 fb⁻¹
 PLB 829 (2022) 137066
- $E_T^{\text{miss}} + Z(q\bar{q})$, 36.1 fb⁻¹
 JHEP 10 (2018) 180
- $E_T^{\text{miss}} + tW$, 139 fb⁻¹
 arXiv:2211.13138
- $E_T^{\text{miss}} + j$, 139 fb⁻¹
 PRD 103 (2021) 112006
- $tbH^\pm(tb)$, 139 fb⁻¹
 JHEP 06 (2021) 145
- $t\bar{t}t$, 139 fb⁻¹
 arXiv:2211.01136
- $h \rightarrow$ invisible, 139 fb⁻¹
 arxiv:2301.10731

Scenario 1a: $\sin \theta = 0.35$ m_A - m_a plane

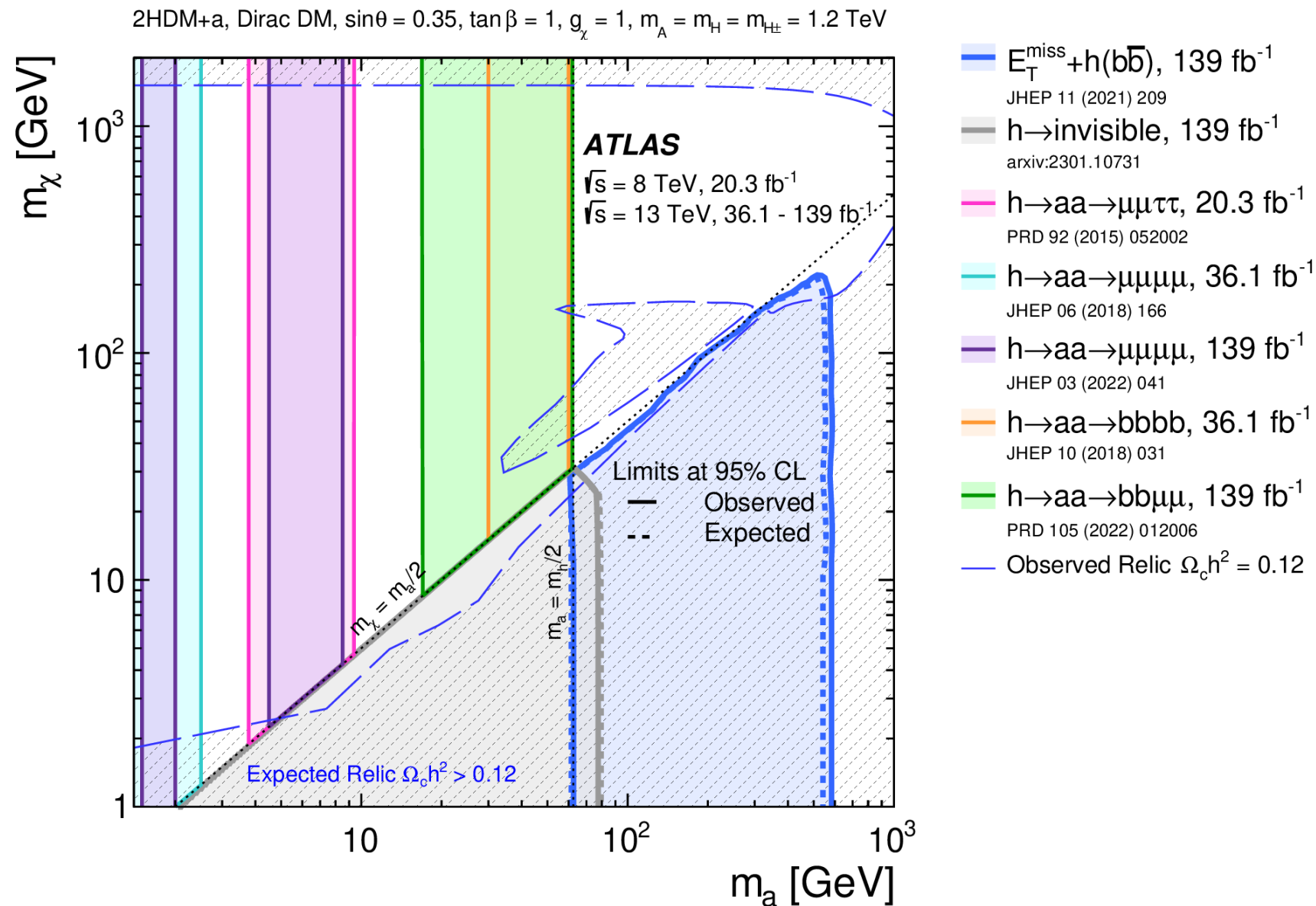
- $h \rightarrow$ invisible constrains very low m_a .
- constraints from $E_T^{\text{miss}} + h$ signatures: similar m_A - m_a dependence, with $h \rightarrow bb$ most sensitive.
- $E_T^{\text{miss}} + tW$ similar to $E_T^{\text{miss}} + Z(\ell\ell)$ but with smaller excl. region.
- $E_T^{\text{miss}} + \text{jet}$ sensitivity notably different from those of $E_T^{\text{miss}} + Z$ and $E_T^{\text{miss}} + h$.
- Complementary constraints from searches not targeting DM.
- Sensitivity of 2HDM+a driven by the combination.



Most comprehensive
 set of constraints on
 2HDM+a to date

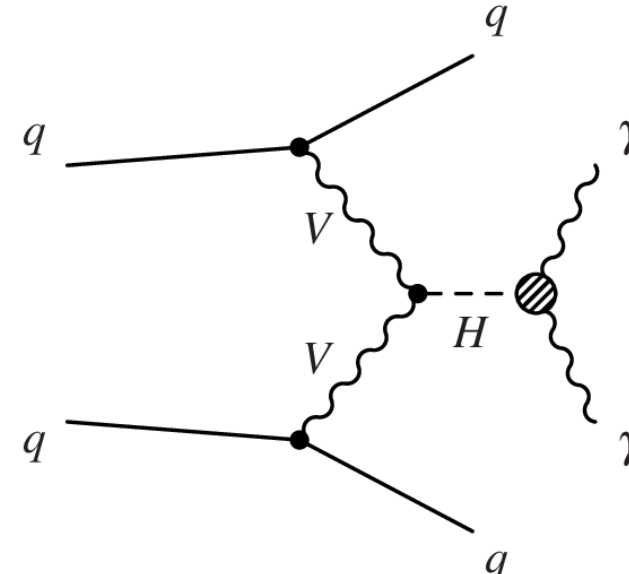
Scenario 6: m_a - m_χ plane

- New interpretation in m_a - m_χ plane:
 - Searches for SM Higgs decaying to 4 fermions via aa constrain previously unprobed region of 2HDM+a.
 - Complementarity to $h \rightarrow$ invisible and $E_T^{\text{miss}} + h(bb)$ searches.



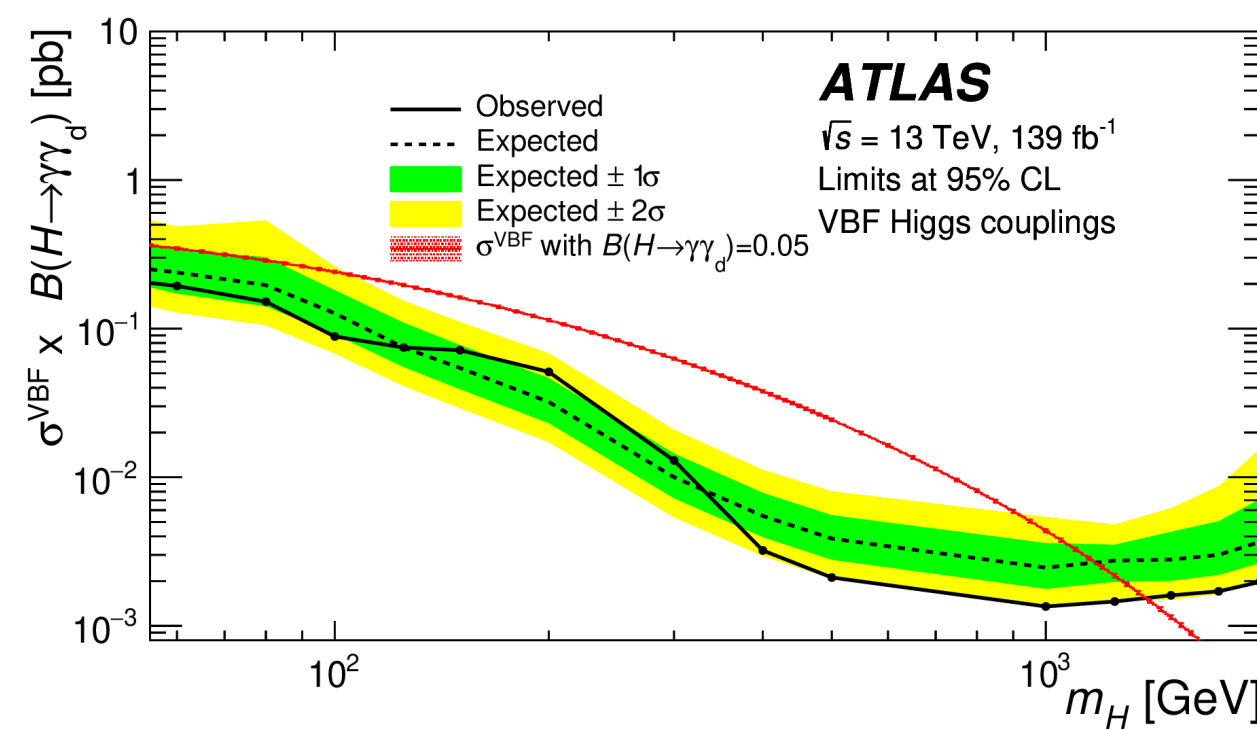
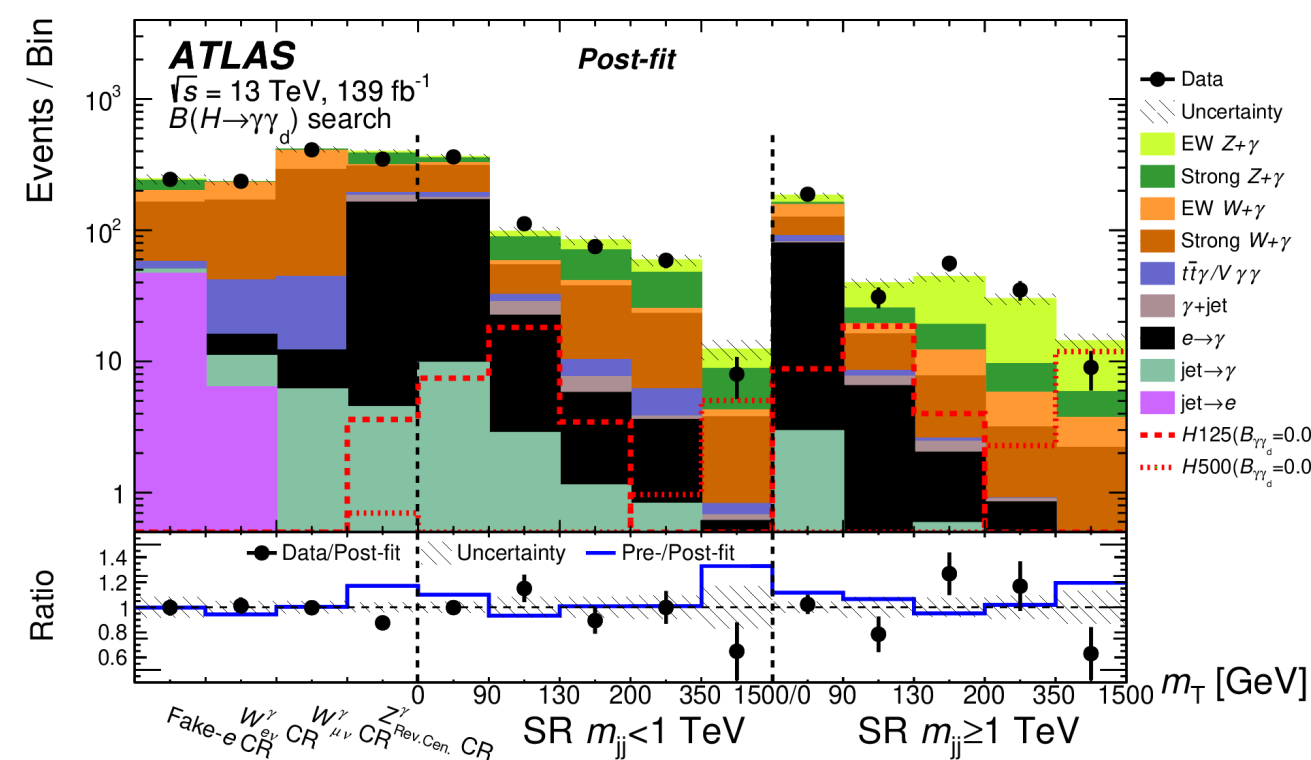
II. Recent ATLAS $H \rightarrow \gamma\gamma_d$ searches in resonant $\gamma + E_T^{\text{miss}}$ signature

VBF $H \rightarrow \gamma\gamma_d$



- search for $H \rightarrow \gamma\gamma_d$ with VBF production mode
 - $m_H \in [60, 2000]$ GeV; massless dark photon;
 - dark photon collider stable $\rightarrow E_T^{\text{miss}}$;
 - final state with 1 photon, jets and E_T^{miss} .
- Signal region: single-photon trigger, isolated photon, 2 forward jets with $|\Delta\eta_{jj}| > 2.5$, high E_T^{miss} .
- SR and CRs divided into 2 bins of m_{jj} with 5 bins of $m_T(\gamma, E_T^{\text{miss}})$ each.
- ggF $H \rightarrow \gamma\gamma_d$ signal contribution included for 125 GeV Higgs.

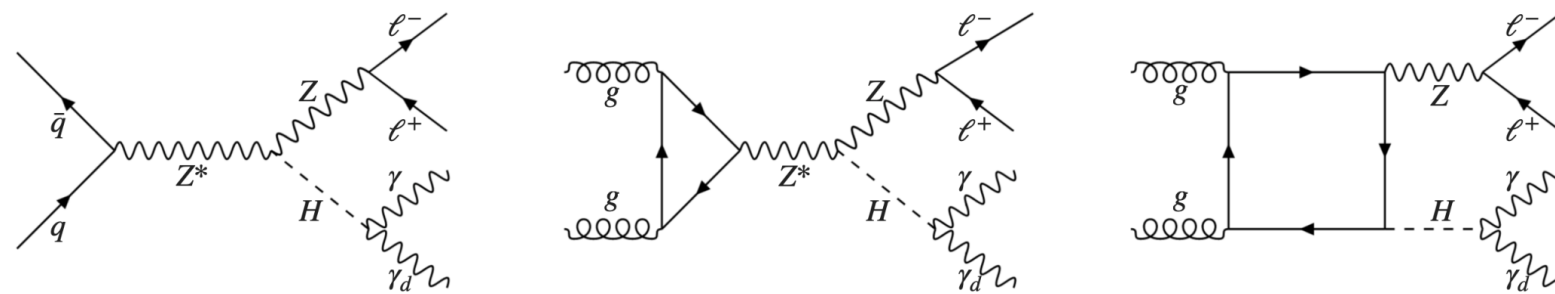
An **observed (expected) 95% CL upper limit on BR** is set at **1.8 (1.7) %**, assuming **SM 125 GeV Higgs boson and massless dark photon**.



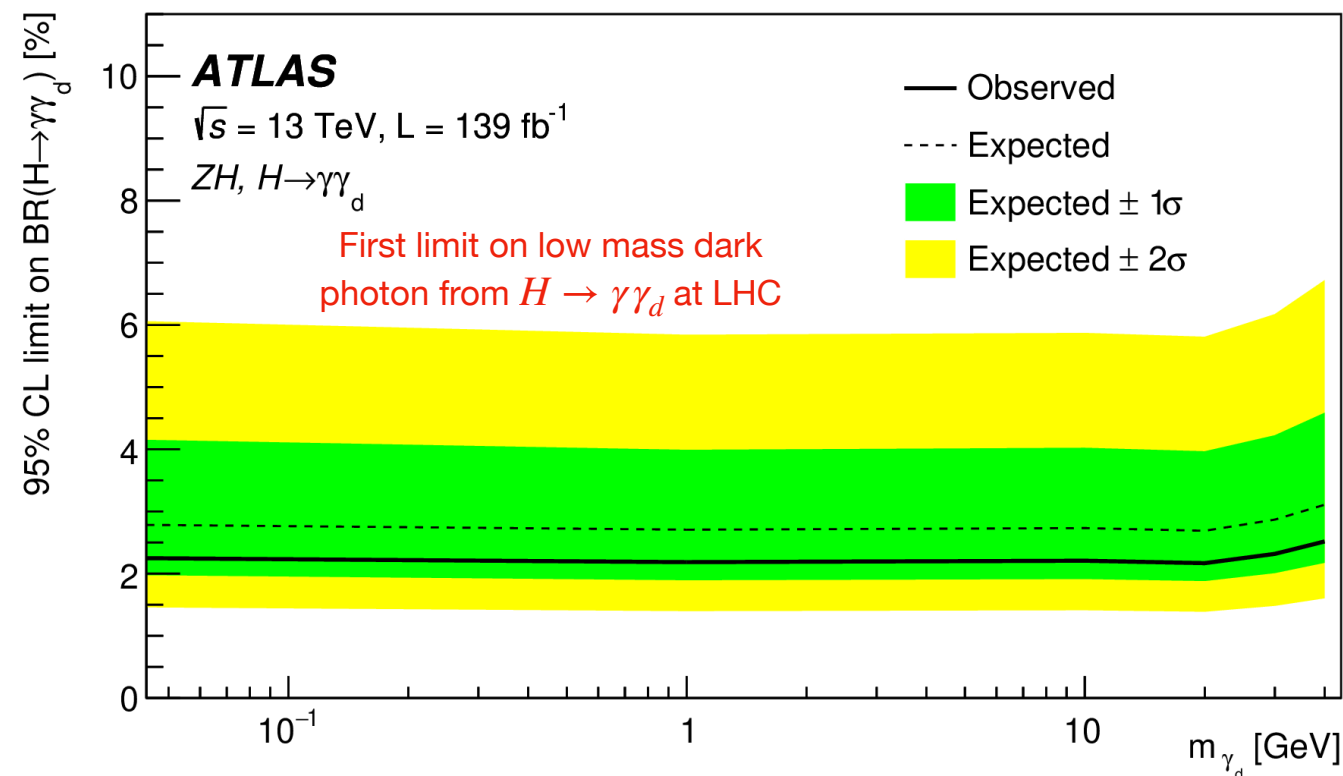
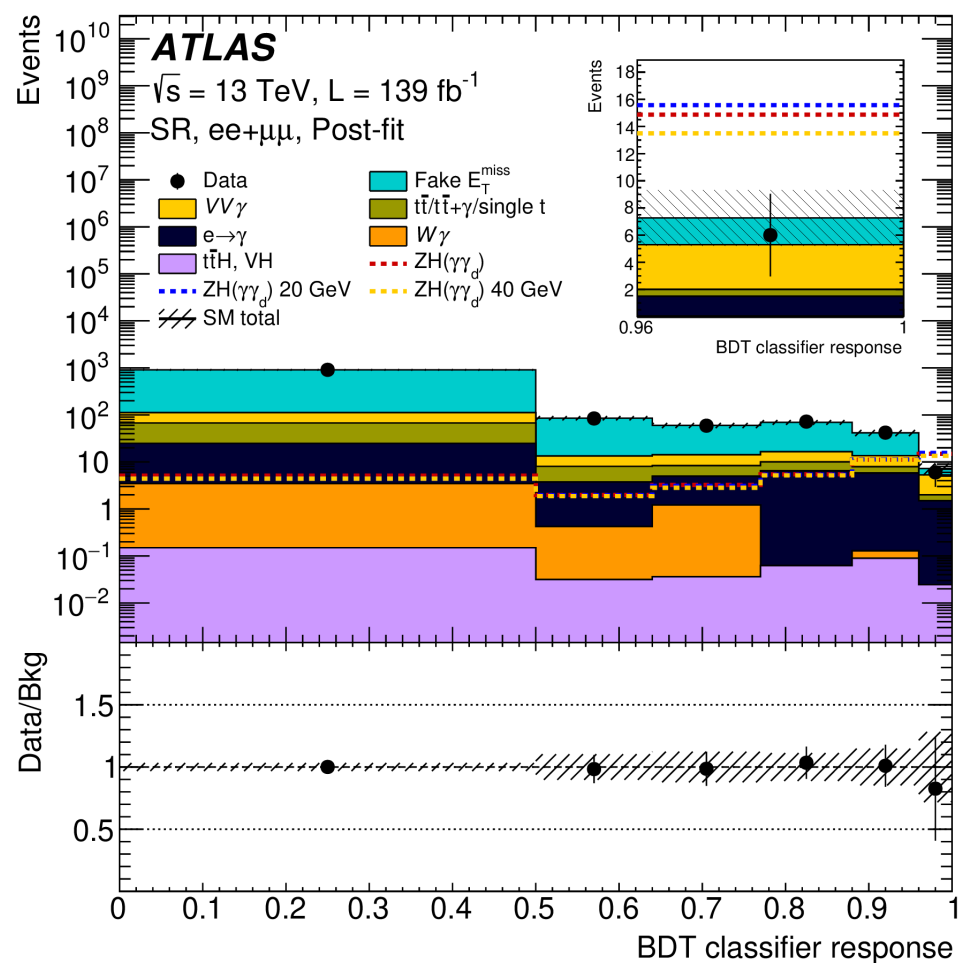
ZH, $H \rightarrow \gamma\gamma_d$

- Search for $H \rightarrow \gamma\gamma_d$ with ZH production mode

- $m_H = 125$ GeV; $m_{\gamma_d} \in [0, 40]$ GeV;
- dark photon $\rightarrow E_T^{\text{miss}}$; $Z \rightarrow l^+l^-$;



- BDT (XGBOOST) optimised specifically for 125 GeV Higgs, used to enhance sensitivity.



Production	ZH	VBF
ATLAS	2.3 (2.8)%	1.8 (1.7)%
CMS	4.6 (3.6)%	3.5 (2.8)%

Prospects for statistical combination

- Combination of VBF and ZH channels for **SM Higgs (125 GeV)** decaying into photon and **massless dark photon**

Production	ZH	VBF	Combined
ATLAS	2.3(2.8)%	1.8(1.7)%	Our ongoing work
CMS	4.6(3.6)%	3.5(2.8)%	2.9(2.1)%

Observed and expected 95% CL limits at $m_H = 125$ GeV

- Combination of VBF and **ATLAS mono-photon re-interpretation** for **heavy Higgs** decaying into photon and **massless dark photon**. (Our ongoing work)

Conclusion

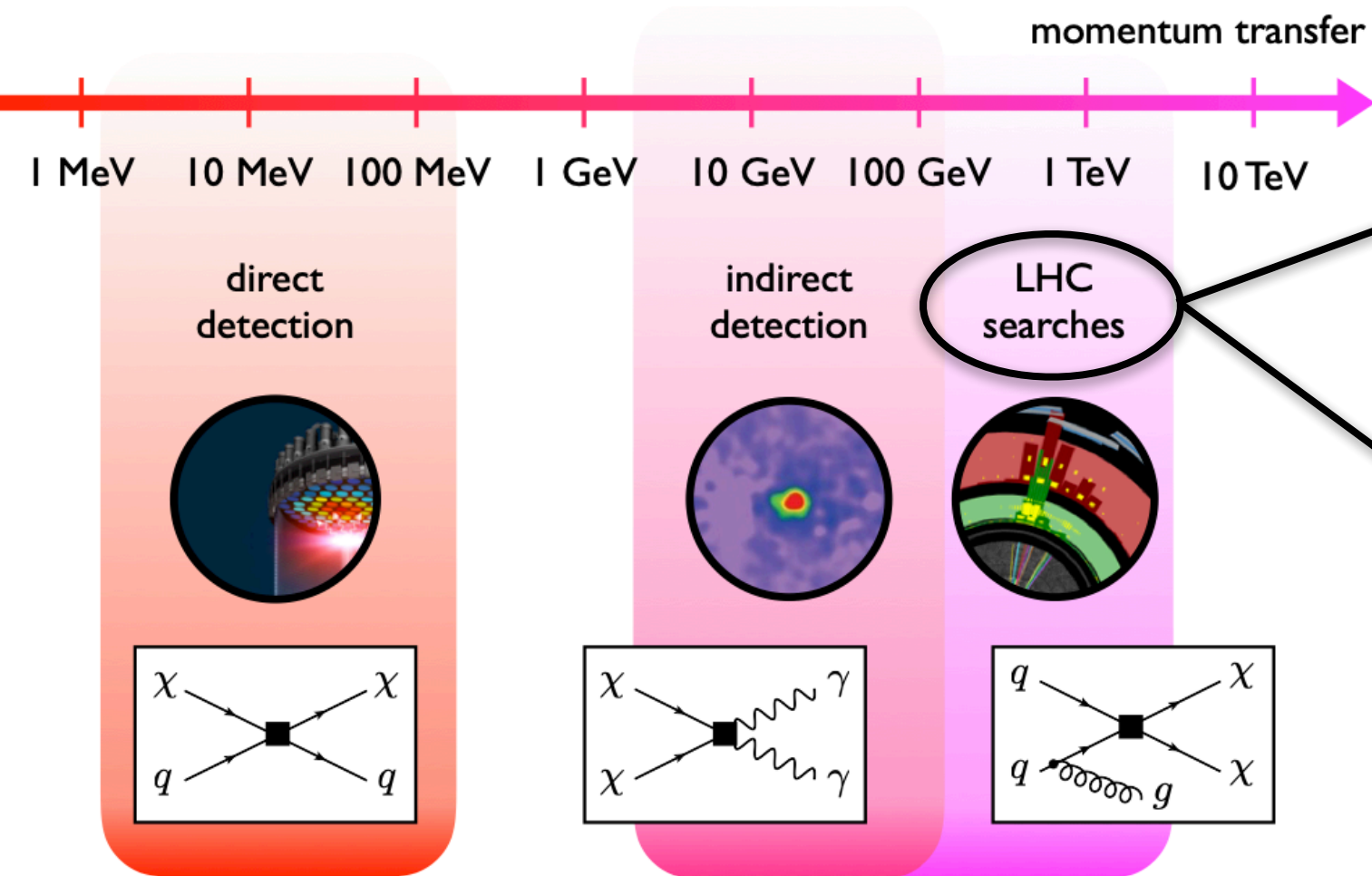
- Most comprehensive set of constraints on the 2HDM+a obtained by the ATLAS to date; determine sensitivity of many relevant signatures, some obtained for the first time.
- Statistical combination of $E_T^{miss} + Z(ll)$, $E_T^{miss} + h(bb)$ and $tbH^\pm(tb)$ extends the sensitivity to the 2HDM+a compared to the sensitivities derived from the individual searches across different regions of the 2HDM+a parameter space
- For the first time the results of searches targeting $h \rightarrow aa \rightarrow 4f$ are used to constrain a part of previously unprobed 2HDM+a parameter space.
- Upper limit on $\text{Br}(H \rightarrow \gamma\gamma_d)$ of 1.8% obtained in VBF, $H \rightarrow \gamma\gamma_d$ search, for **SM 125 GeV Higgs boson** and **massless dark photon**: the most stringent limit from experiment so far.
- Ongoing work for stat. combination to extend constraints on $\text{Br}(H \rightarrow \gamma\gamma_d)$ for both SM Higgs and heavy Higgs cases.

Thank you for your attention!!!

Backup

DM collider searches

- Dark Matter: supported by many of astrophysical measurements; SM is insufficient to explain → strong consideration in many BSM extensions.
- Complementary probes of DM in several areas



- ATLAS sensitive to wide variety of DM, especially WIMPs.
 - relic density → WIMP mass \sim EWK scale.
- provide access to nature of DM \leftrightarrow SM interaction (*mediator*), via
 - $E_T^{\text{miss}} + X$ (mono- X , mediator \rightarrow invisible)
 - Resonance / decay product reconstruction (mediator \rightarrow visible).

E_T^{miss} : missing transverse momentum

2HDM+a

- Coupling of pseudo scalar P to the dark Dirac fermion χ

$$\mathcal{L}_\chi = -iy_\chi P \bar{\chi} \gamma_5 \chi ,$$

- Yukawa couplings of Higgs doublets to SM fermions

$$\mathcal{L}_Y = - \sum_{i=1,2} \left(\bar{Q} Y_u^i \tilde{H}_i u_R + \bar{Q} Y_d^i H_i d_R + \bar{L} Y_\ell^i H_i \ell_R + \text{h.c.} \right) .$$

- Most general scalar potential of two Higgs doublets

$$V = V_H + V_{HP} + V_P ,$$

$$V_H = \mu_1 H_1^\dagger H_1 + \mu_2 H_2^\dagger H_2 + \left(\mu_3 H_1^\dagger H_2 + \text{h.c.} \right) + \lambda_1 (H_1^\dagger H_1)^2 + \lambda_2 (H_2^\dagger H_2)^2 \\ + \lambda_3 (H_1^\dagger H_1) (H_2^\dagger H_2) + \lambda_4 (H_1^\dagger H_2) (H_2^\dagger H_1) + \left[\lambda_5 (H_1^\dagger H_2)^2 + \text{h.c.} \right] ,$$

$$V_{HP} = P \left(ib_P H_1^\dagger H_2 + \text{h.c.} \right) + P^2 \left(\lambda_{P1} H_1^\dagger H_1 + \lambda_{P2} H_2^\dagger H_2 \right) ,$$

$$V_P = \frac{1}{2} m_P^2 P^2 .$$

$E_T^{\text{miss}} + tW$ signature

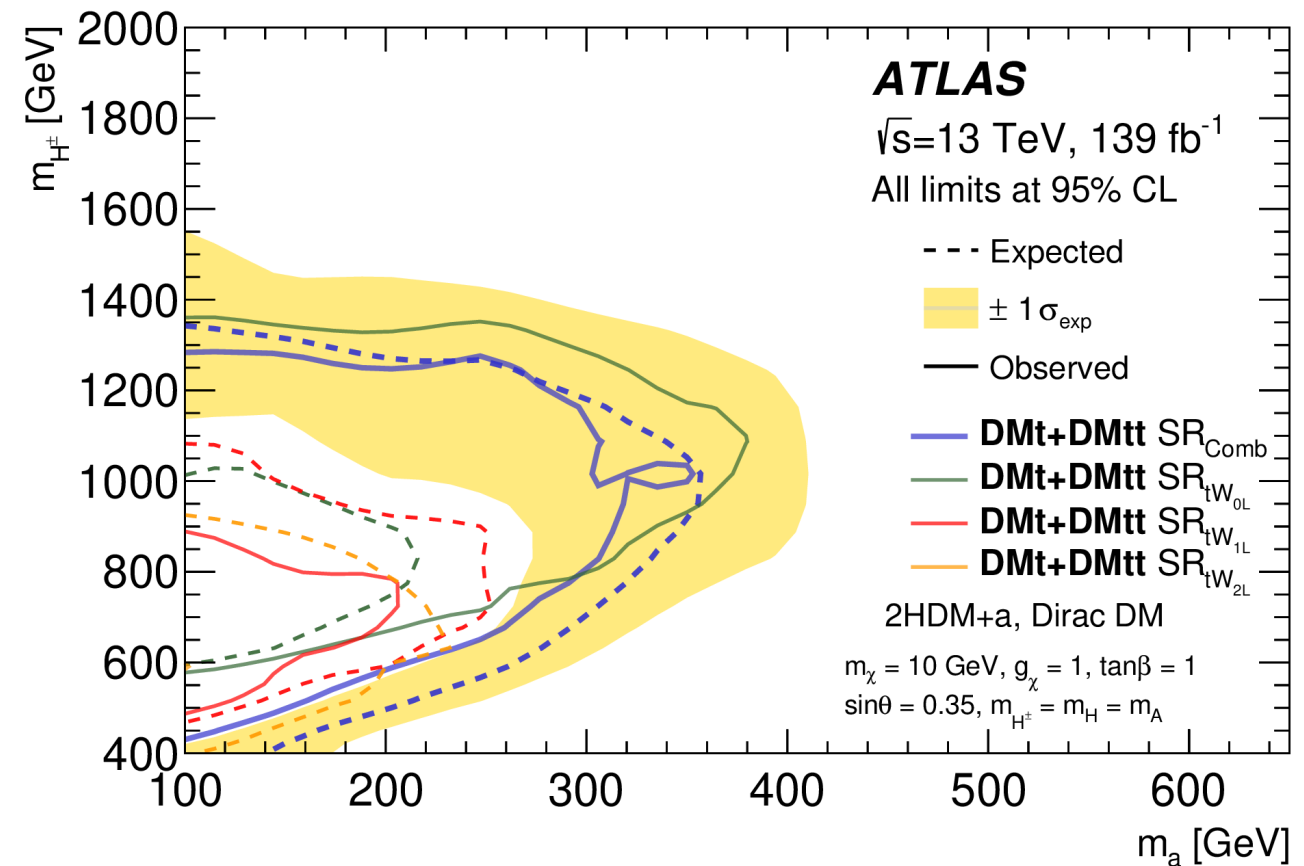
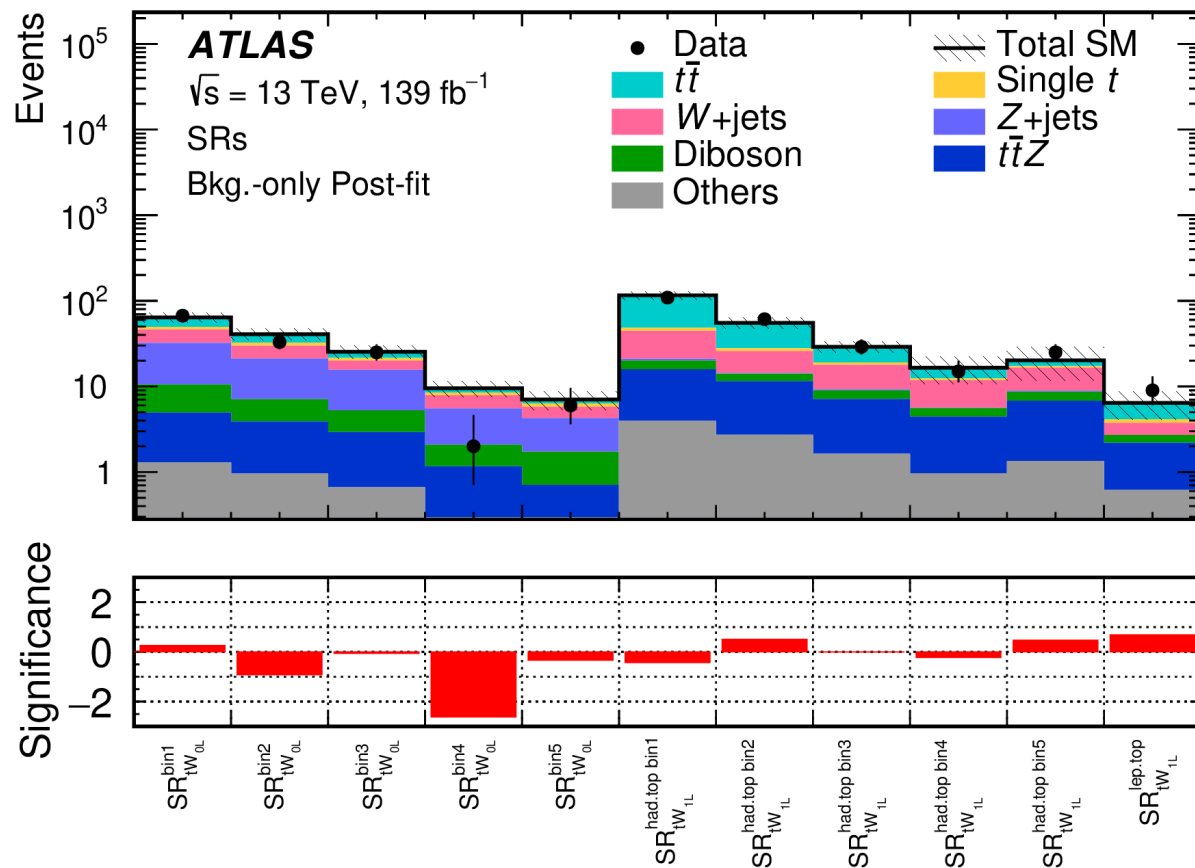
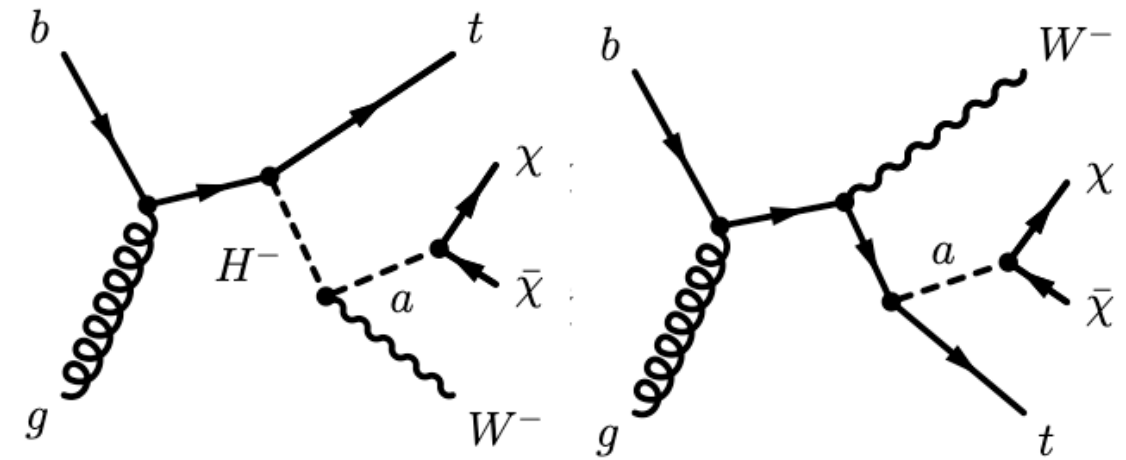
(0- and 1-lepton)

[Eur. Phys. J. C 83 \(2023\) 603](#)

(2-lepton)

[Eur. Phys. J. C 81 \(2021\) 860](#)

- optimised specifically for 2HDM+a and particularly sensitive to on-shell $H^\pm \rightarrow W^\pm a(\chi\bar{\chi})$
- Final interpretations
 - include both 2HDM+a $E_T^{\text{miss}} + t\bar{t}$ and $E_T^{\text{miss}} + tW$ signal contributions.
 - with combination of all three 0-, 1-, and 2-lepton channels.



HLRS searches

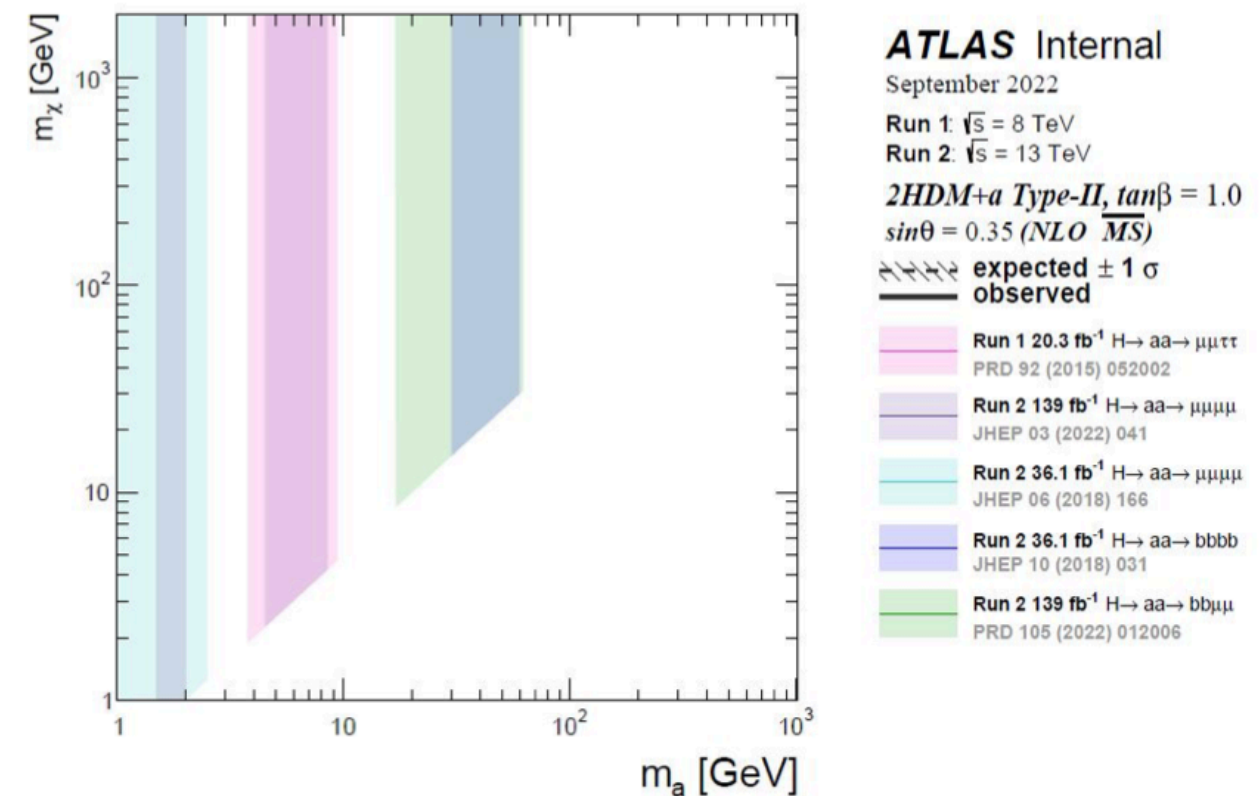
For lower values of m_a , there is strong complementarity with light resonance searches for $H \rightarrow aa \rightarrow 4f$. A $m_a - m_\chi$ scan has been designed to illustrate that.

Benchmark model parameters tuned to evade constraints from total Higgs width:

$$\{m_A, \tan \beta, \sin \theta, \lambda_3, y_\chi\} = \{1.2 \text{ TeV}, 1, 0.35, 3, 1\}$$

Results from the following searches are used as inputs for $m_a - m_\chi$ scan:

- search for $H \rightarrow aa \rightarrow bb\mu\mu$ [[arXiv:2110.00313](https://arxiv.org/abs/2110.00313)]
- search for $H \rightarrow aa \rightarrow bbbb$ [[arXiv:1806.07355](https://arxiv.org/abs/1806.07355)]
- two searches of the $H \rightarrow XX/ZX \rightarrow llll$ [[arXiv:1802.03388](https://arxiv.org/abs/1802.03388), [arXiv:2110.13673](https://arxiv.org/abs/2110.13673)]
- search for $H \rightarrow aa \rightarrow \mu\mu\tau\tau$ [[arXiv:1505.01609](https://arxiv.org/abs/1505.01609)]

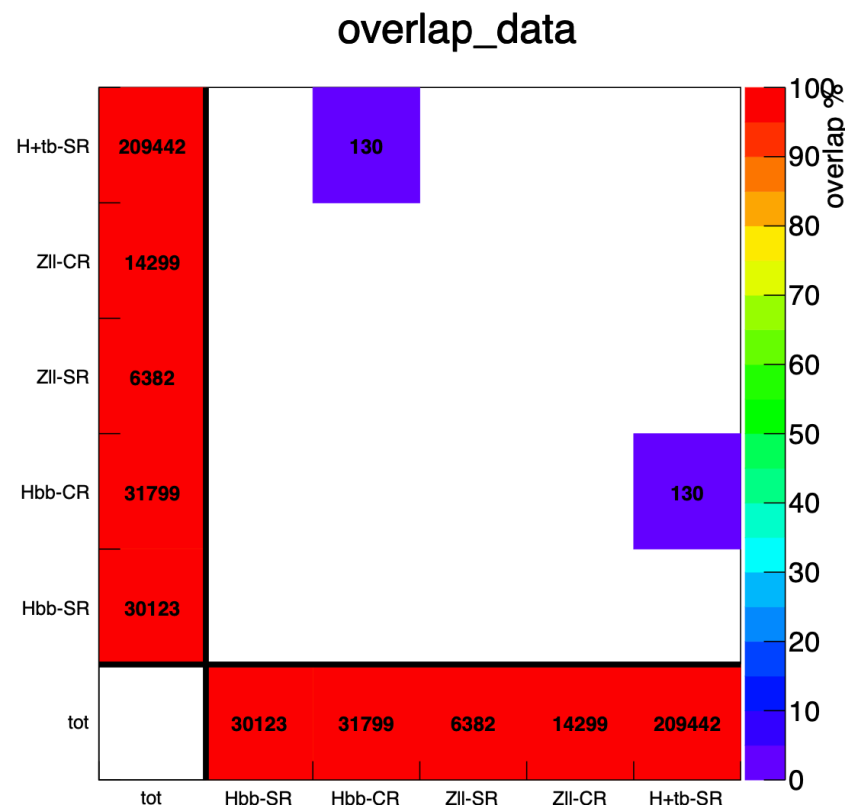


Statistical combination of results

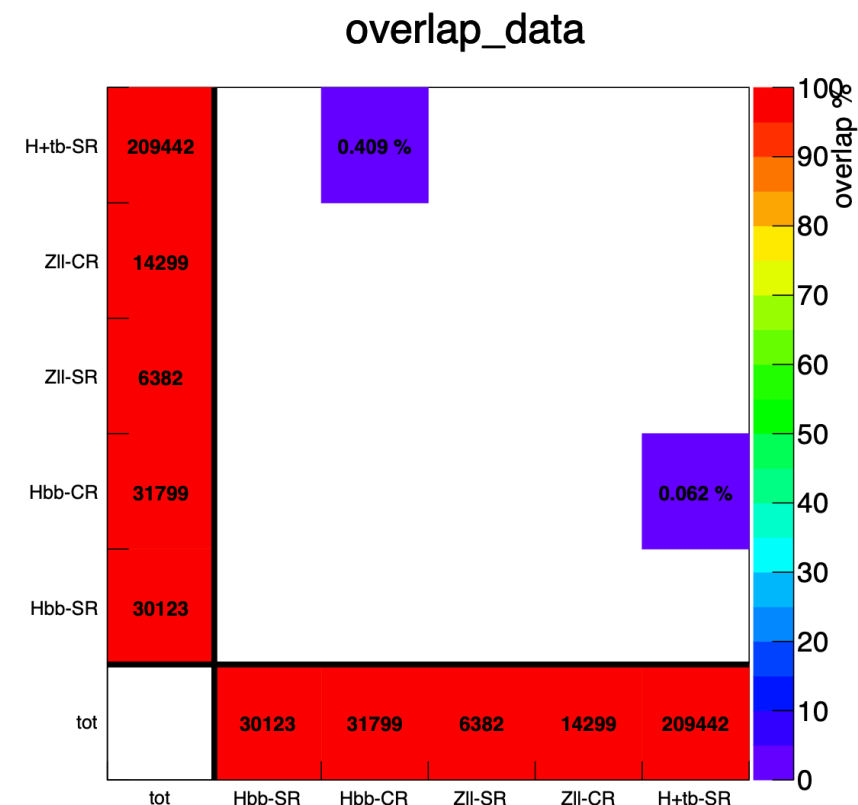
Orthogonality checks

- The statistical combination is facilitated as the input analyses statistically independent.
- Due to b- and lepton-multiplicity requirements, no overlap between the 3 analyses SRs is expected.
- Negligible ($\ll 1\%$) event overlap observed between $H^\pm \rightarrow tb$ SR and $E_T^{miss} + h(bb)$ CR, no impact on the combination.

Input Analysis	Signal selection
EtMiss + Z(l)	b-jet veto
EtMiss + h(bb)	≥ 2 b-jets, 0 lepton
Charged H \rightarrow tb	≥ 3 b-jets, 1 lepton



(a) Full run 2 data, number of overlapped events



(b) Full run 2 data, fraction of overlapped events

Statistical combination of results

Statistical analysis

- The combination is performed by constructing the analyses' likelihood and maximizing the corresponding profile likelihood ratio.
- The likelihood used in the combination defined as:

$$\mathcal{L}(\text{data}|\mu, \lambda_\mu, \theta_\mu) = \prod_{c=1}^{N_{\text{cats}}} \mathcal{L}_c(\text{data}|\mu, \lambda_\mu, \theta_\mu) \prod_{k=1}^{N_{\text{cons}}} \mathcal{F}(\tilde{\theta}_{\mu,k}|\theta_{\mu,k})$$

Parameter of interest: signal strength Norm factors Nuisance parameters Global observable

Poisson/Gaussian/Log-normal distribution

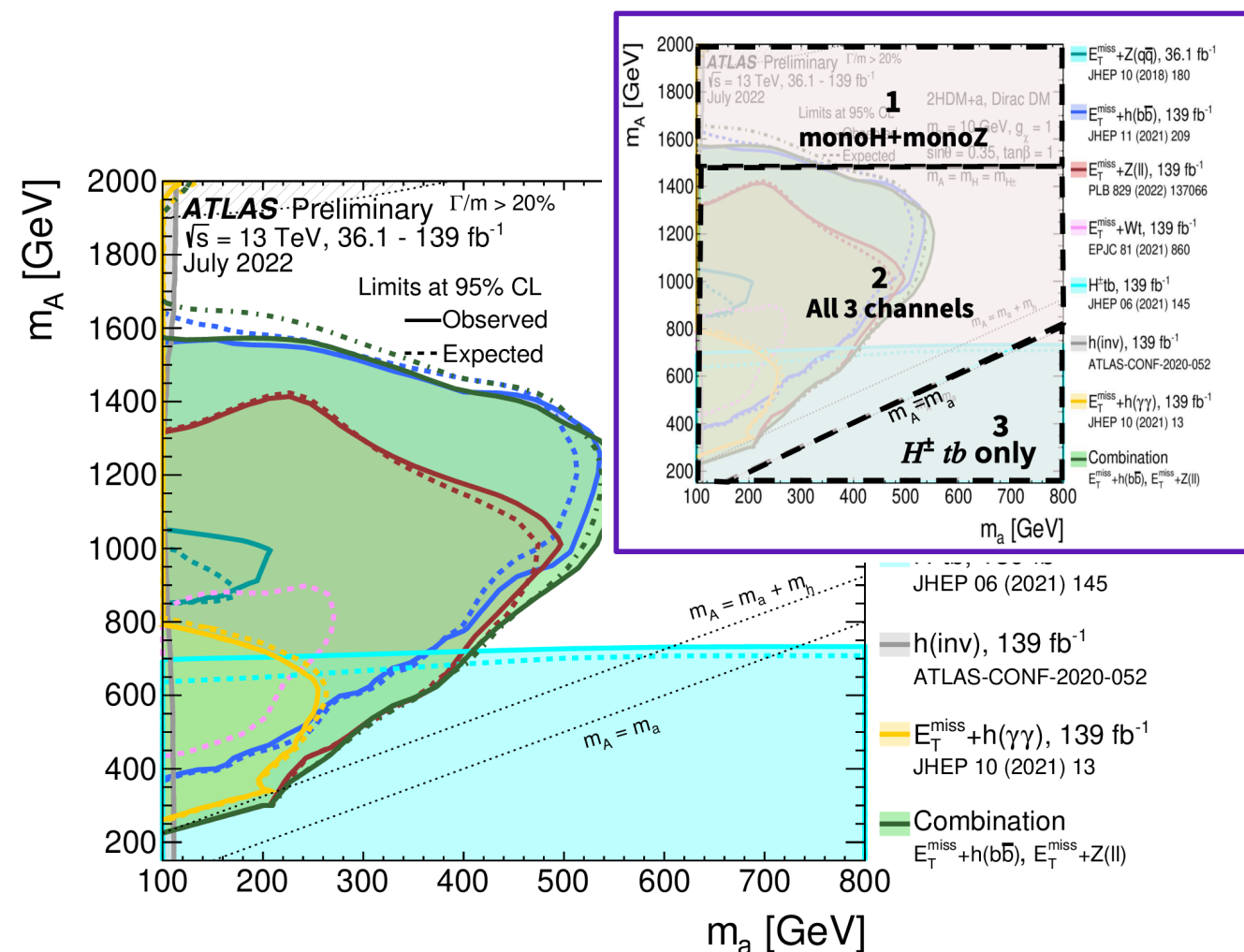
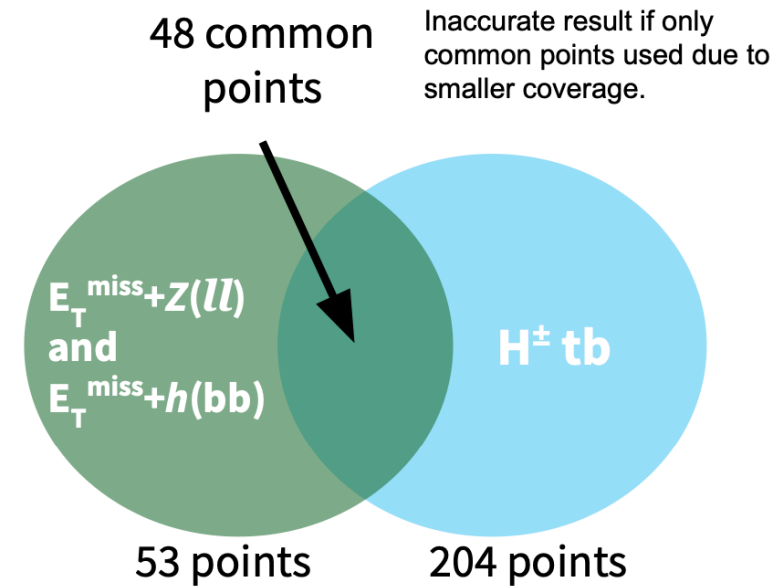
- 95% CL limits are obtained using the profile likelihood ratio test statistic as:

$$q_\mu = \frac{\mathcal{L}(\mu, \hat{\lambda}_\mu, \hat{\theta}_\mu)}{\mathcal{L}(\hat{\mu}, \hat{\lambda}_{\hat{\mu}}, \hat{\theta}_{\hat{\mu}})},$$

Statistical combination of results

Combination strategy

- $tbH^\pm(tb)$ added to stat. combination with $E_T^{miss} + Z(ll)$ and $E_T^{miss} + h(bb)$ for the first time \rightarrow can significantly improve sensitivity.
- Usually, the combination is done for every common signal point over 3 channels.
 - **Hybrid combination approach:** exclude channels that have negligible sensitivities in a certain region.
 - $m_A > 1500$ GeV: $E_T^{miss} + Z(ll)$ and $E_T^{miss} + h(bb)$.
 - $m_A < 1500$ GeV and $m_A > m_a$: all 3 channels combined.
 - $m_A < m_a$ (off-shell region for mono-X searches): $H^\pm \rightarrow tb$ only.



Statistical combination of results

Uncertainties and their correlations

- Most experimental uncertainties related to reconstruction of physics objects are correlated across search channels.
- Uncertainties stemming from b-jet identification are not correlated due to different choices of algorithm and operating point.
- Uncertainties constrained in a particular analysis are not correlated to avoid bringing tensions from any phase-space-specific biases across channels.
- Due to different processes and phase spaces being probed, modelling uncertainties are uncorrelated across analyses.
- Different correlation choices for FTAG/JER/MET and strongly-constrained NPs were tested without observed impact on the exclusions.

Uncertainty source	$\Delta\mu$ [%]
Statistical uncertainty	25.0
Systematic uncertainties	27.6
Theory uncertainties	16.2
Signal modelling	2.8
Background modelling	15.9
Experimental uncertainties (excl. MC stat.)	18.8
Luminosity, pile-up	3.9
Jets, E_T^{miss}	12.3
Flavour tagging	9.1
Electrons, muons	6.1
MC statistical uncertainty	9.3
Total uncertainty	37.2

stat. and syst. uncertainties to tot. uncertainty on the best-fit μ for ($m_a = 450$ GeV, $m_H = 800$ GeV, $\tan\beta = 1$ and $\sin\theta = 0.35$) excluded by the combination but is not by any single input analysis

Statistical combination of results

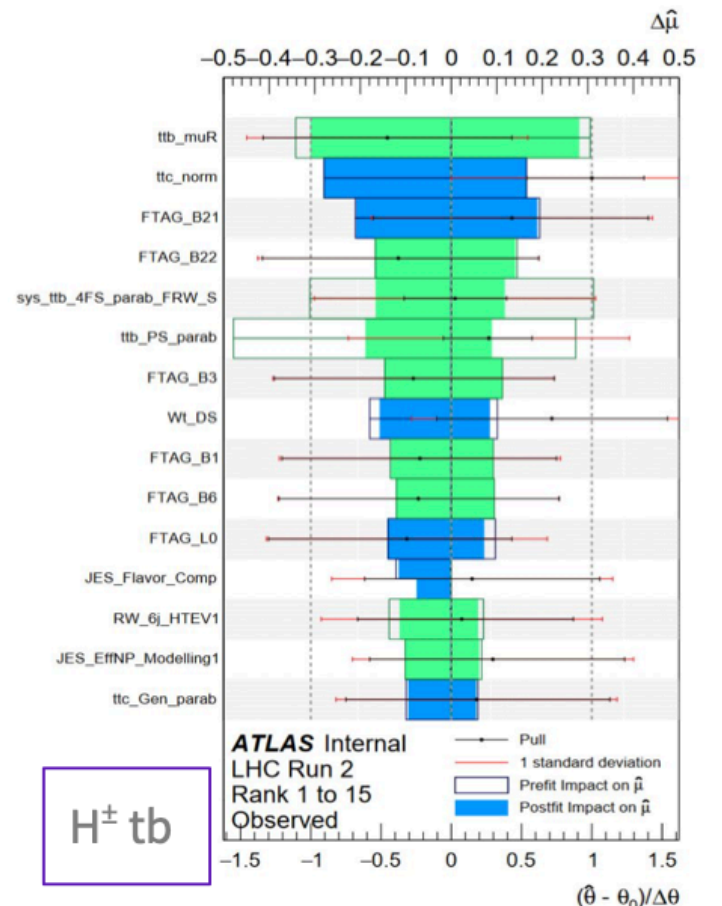
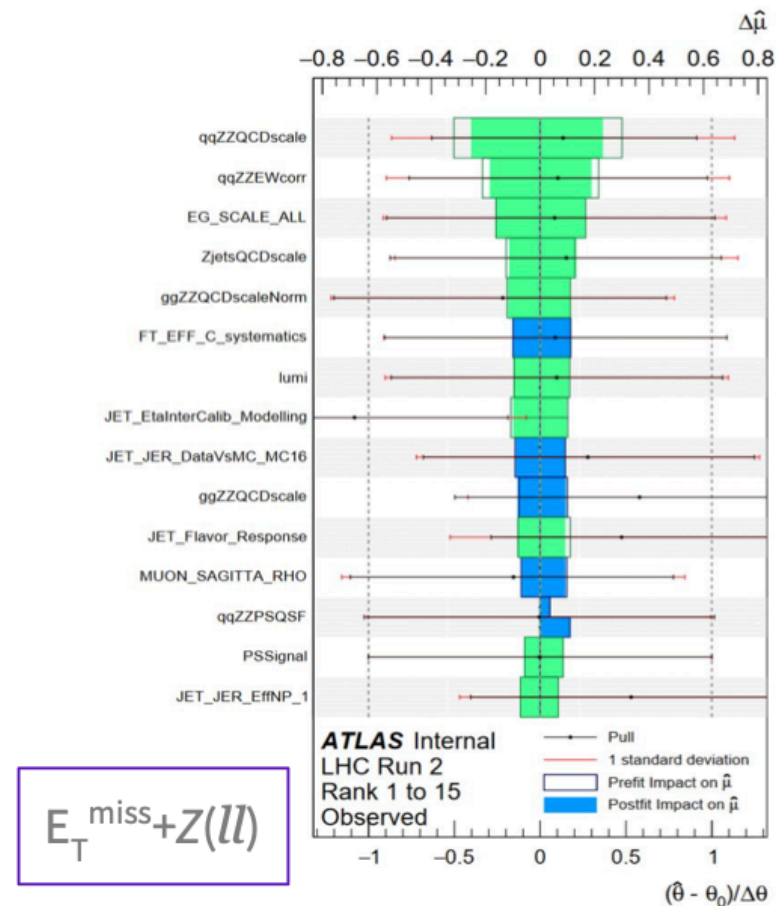
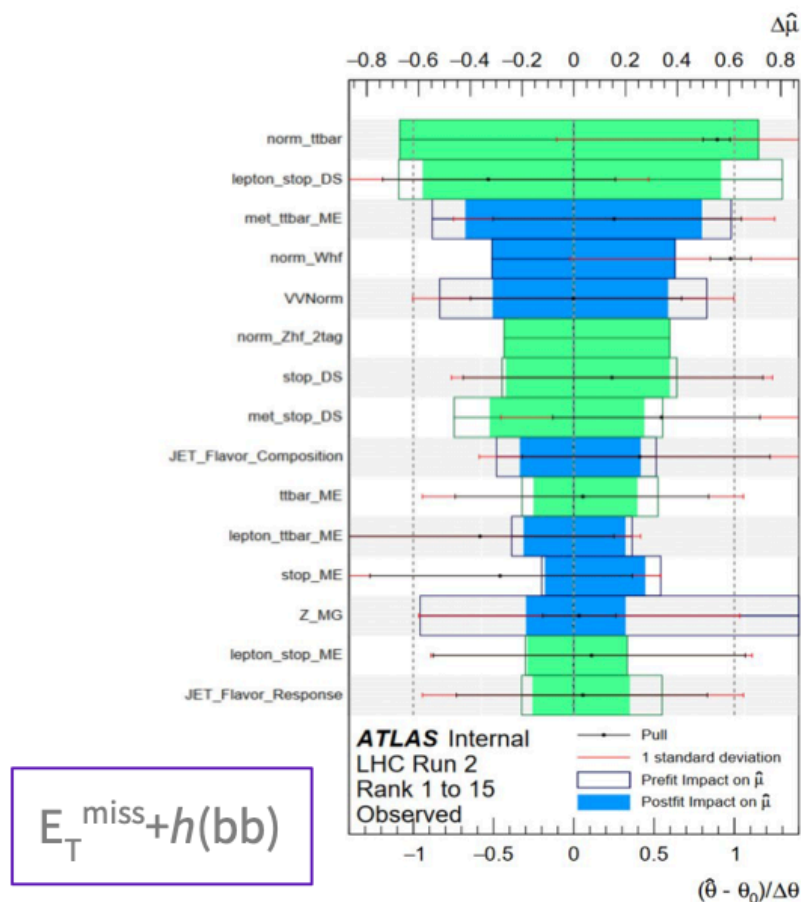
Uncertainties and their correlations

Correlation Scheme

Correlation scheme is studied and developed based on signal at $m_A=800$, $m_a=500$, $\tan\beta=1$ and $\sin\theta=0.35$, in the “intersection” region where it has not been excluded in all three channels but within the reach of sensitivity from combination.

NP rankings for single channels could be reproduced.

The majority of leading NPs are channel-specific systematics (e.g., theory systematics on the background modeling). The impact from correlation should be small.

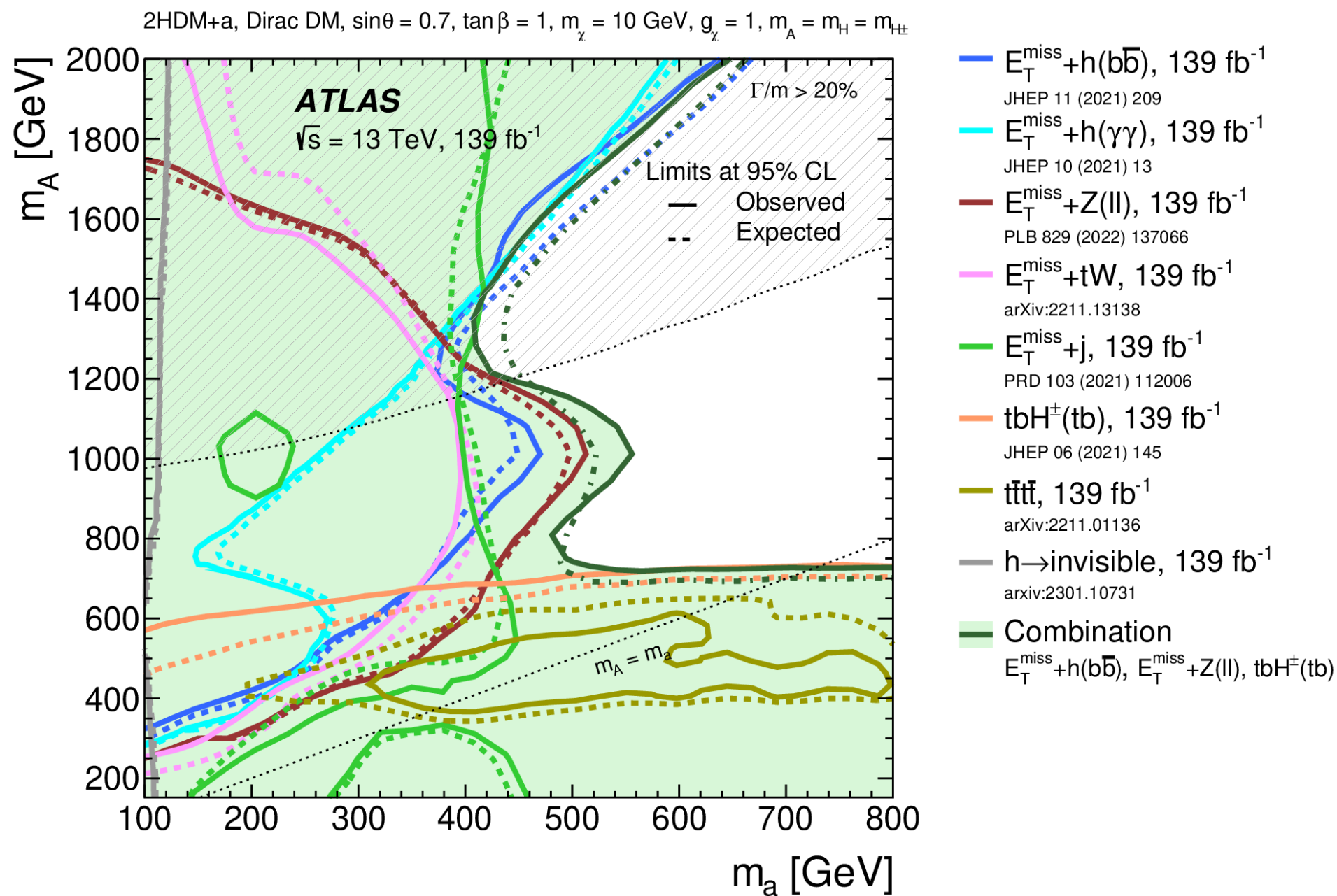


Summary of constraints on 2HDM+a

Variety of searches interpreted in the context of different 2HDM+a benchmark scenarios

Analysis/Scenario	1a	1b	2a	2b	3a	3b	4a	4b	5	6
$E_T^{\text{miss}} + Z(\ell\ell)$ [74]	x	x	x	x	x	x	x	x	x	
$E_T^{\text{miss}} + h(b\bar{b})$ [75]	x	x	x	x	x	x	x	x	x	x
$E_T^{\text{miss}} + h(\gamma\gamma)$ [84]	x	x			x	x	x	x		
$E_T^{\text{miss}} + h(\tau\tau)$ [78]	x			x						
$E_T^{\text{miss}} + tW$ [77]	x	x	x	x	x	x	x	x		
$E_T^{\text{miss}} + j$ [45]	x	x			x	x	x	x		
$h \rightarrow \text{invisible}$ [86]	x	x			x					x
$E_T^{\text{miss}} + Z(q\bar{q})$ [127]	x						x	x		
$E_T^{\text{miss}} + b\bar{b}$ [128]							x	x		
$E_T^{\text{miss}} + t\bar{t}$ [128,129]							x	x		
$t\bar{t}t\bar{t}$ [85]	x	x	x	x	x	x	x	x	x	
$tbH^\pm(tb)$ [76]	x	x	x	x	x	x	x	x	x	
$h \rightarrow aa \rightarrow f\bar{f}f'\bar{f}'$ [79,80,81,82,83]										x

Scenario 1b: $\sin \theta = 0.7$ m_A - m_a plane

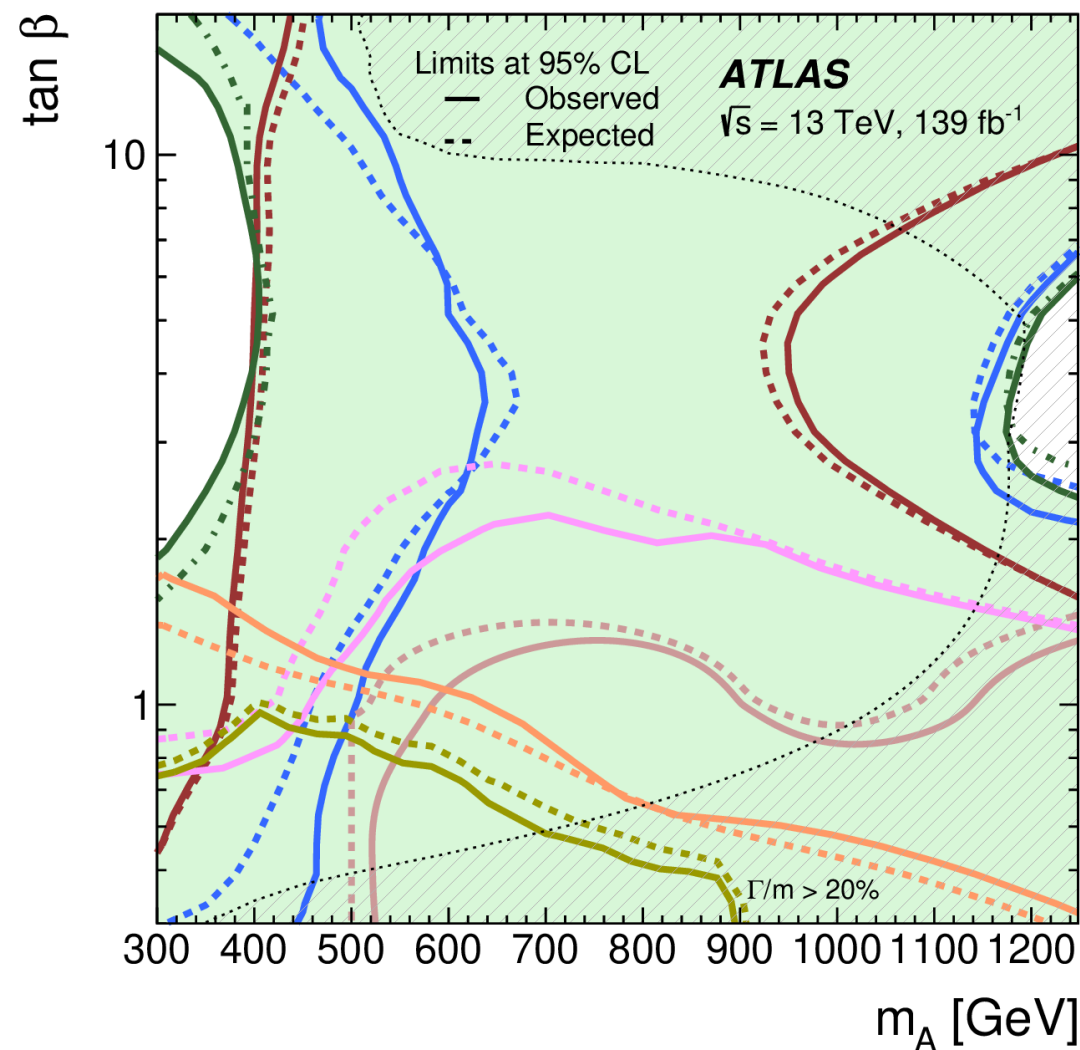
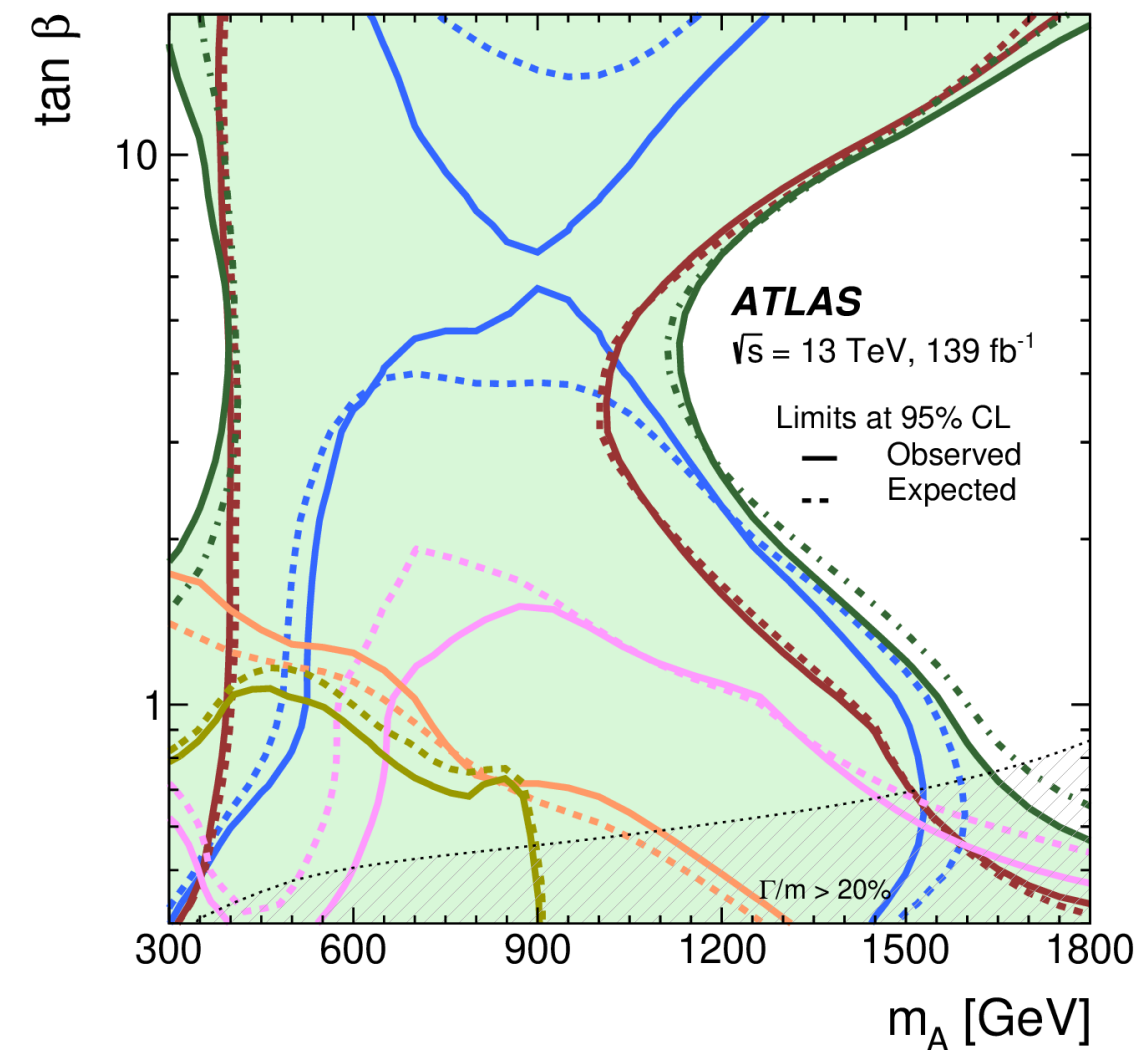


Scenario 2: $m_A - \tan \beta$ planes

- Large fraction of parameter plane excluded by $E_T^{miss} + Z(ll)$, $E_T^{miss} + h(bb)$ dominates in high- m_A but still gives sensitivity in low- m_A with $tbH^\pm(tb)$.
- $E_T^{miss} + Z(ll)$ and $E_T^{miss} + h(bb)$ sensitivities driven by the transition from gg- to bb-initiated production with a decrease at $\tan \beta \approx 5$.
- Combination significantly improves the excl. parameter space.

2HDM+a, Dirac DM, $\sin\theta = 0.35$, $m_\chi = 10$ GeV, $g_\chi = 1$, $m_A = m_H = m_{H^\pm}$, $m_a = 250$ GeV

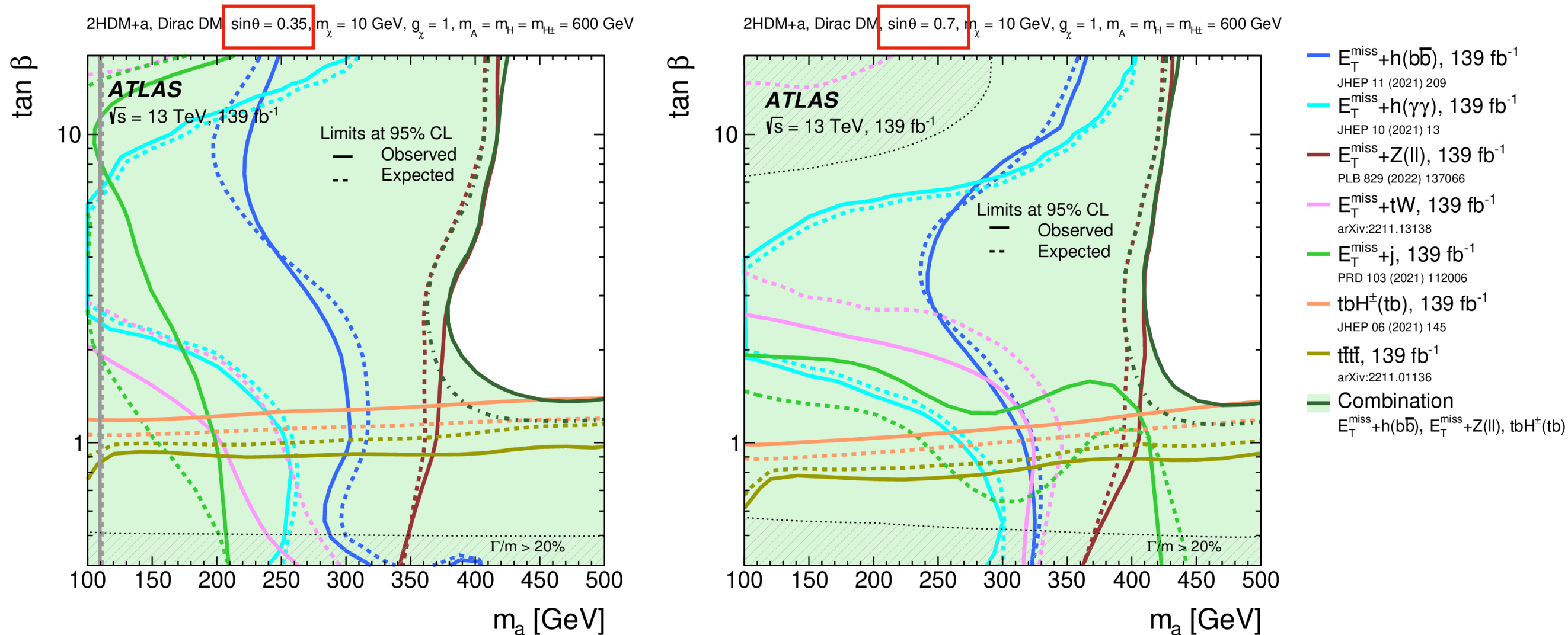
2HDM+a, Dirac DM, $\sin\theta = 0.7$, $m_\chi = 10$ GeV, $g_\chi = 1$, $m_A = m_H = m_{H^\pm}$, $m_a = 250$ GeV



- $E_T^{miss} + h(b\bar{b})$, 139 fb⁻¹
JHEP 11 (2021) 209
- $E_T^{miss} + h(\tau\tau)$, 139 fb⁻¹
arXiv:2305.12938
- $E_T^{miss} + Z(ll)$, 139 fb⁻¹
PLB 829 (2022) 137066
- $E_T^{miss} + tW$, 139 fb⁻¹
arXiv:2211.13138
- $tbH^\pm(tb)$, 139 fb⁻¹
JHEP 06 (2021) 145
- $t\bar{t}t$, 139 fb⁻¹
arXiv:2211.01136
- **Combination**
 $E_T^{miss} + h(b\bar{b})$, $E_T^{miss} + Z(ll)$, tbH^\pm

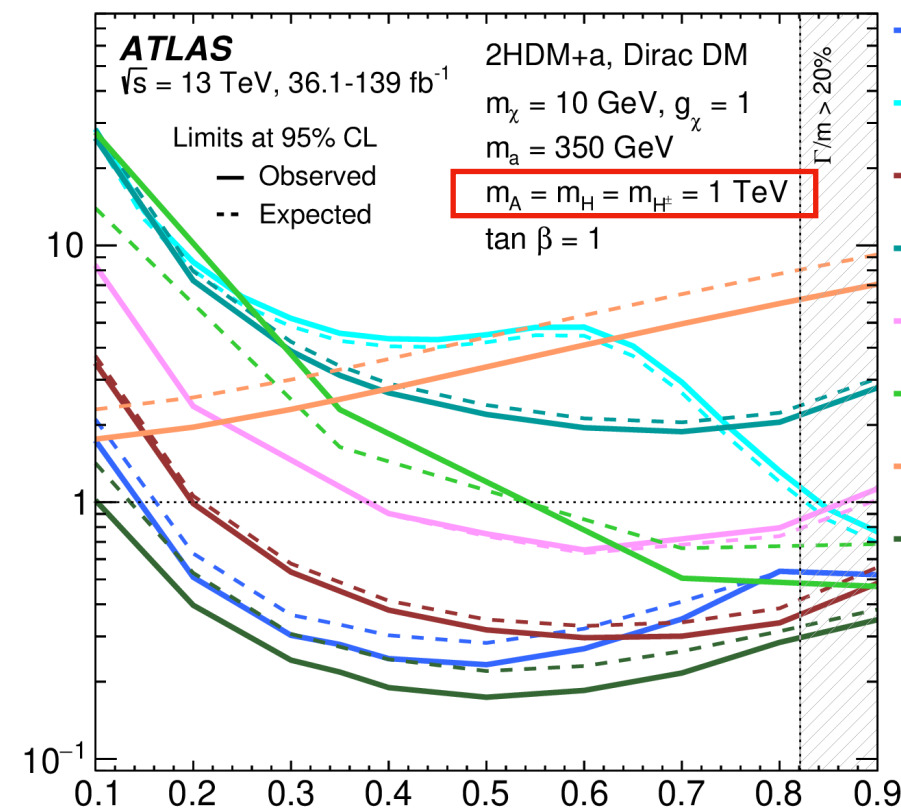
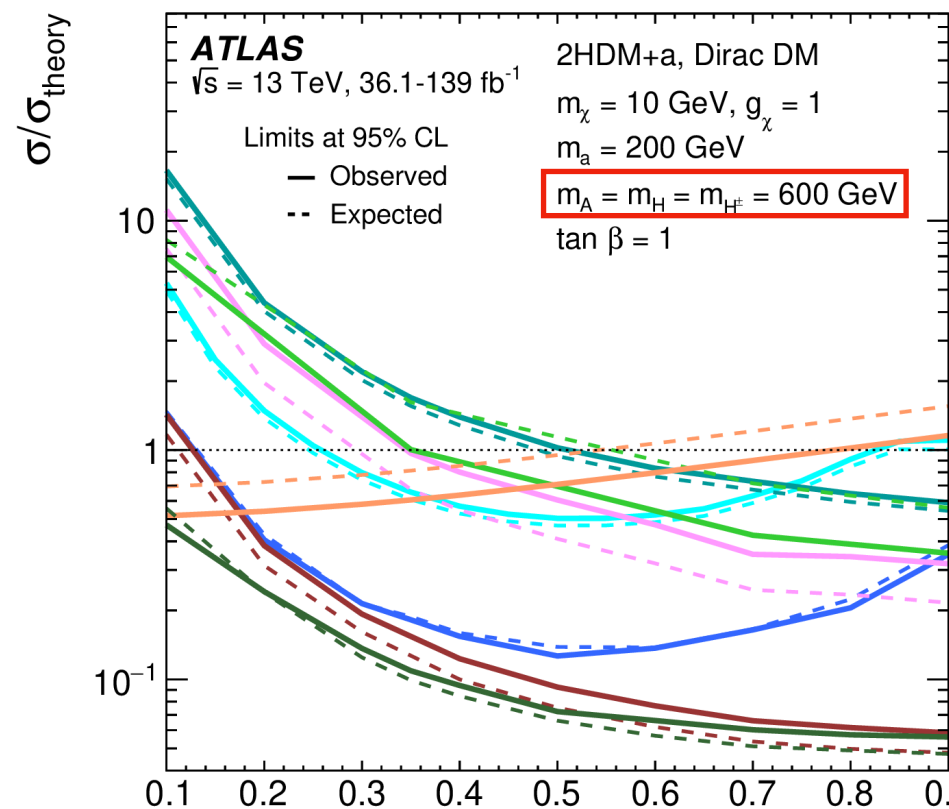
Scenario 3: $m_a - \tan \beta$ planes

- Strongest exclusion from $E_T^{miss} + Z(ll), tbH^\pm(tb)$ is complementary to low- $\tan \beta$ region and moderate dependence on m_a .
- Significant improvement in sensitivity achieved by combination.

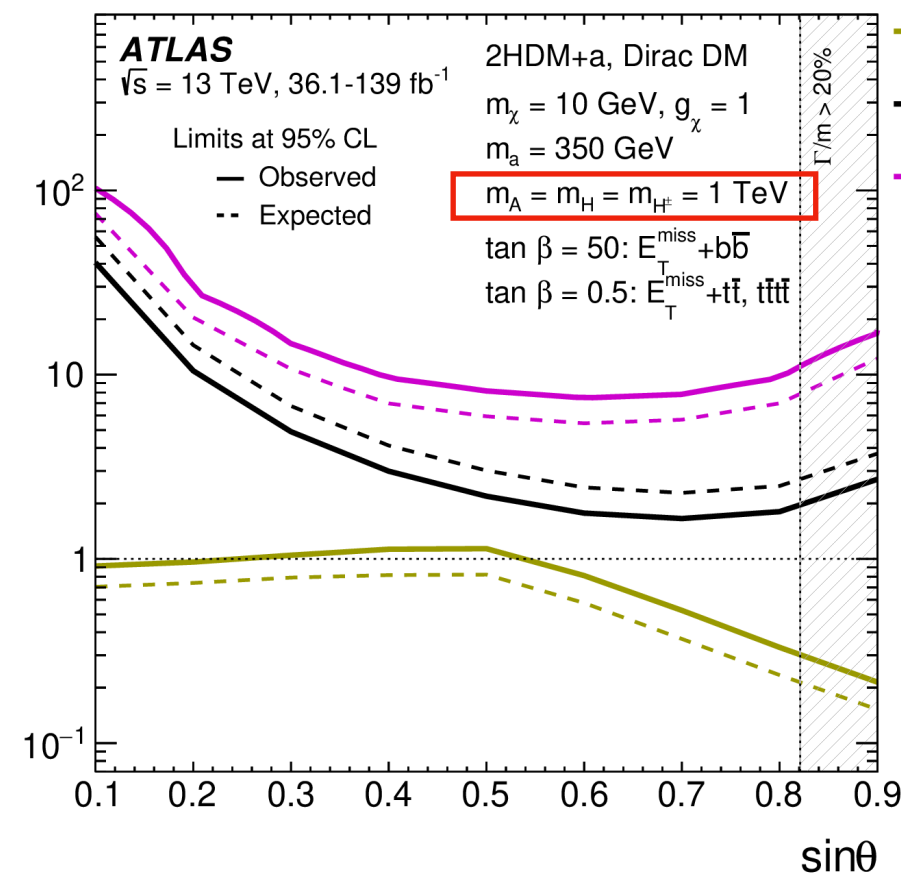
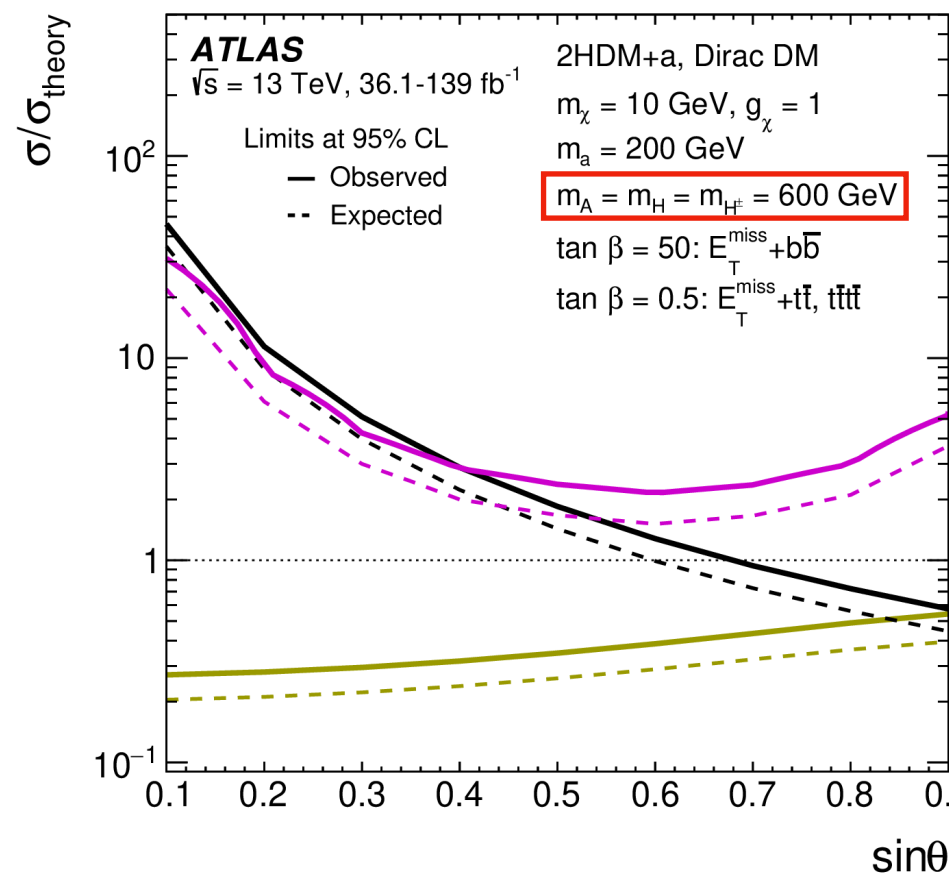


Scenario 4: $\sin \theta$ scans

- $E_T^{miss} + Z(ll)$ and $E_T^{miss} + h(bb)$ provide strongest limits.
- Significant improvement from combination, almost the whole range excluded for these two benchmarks.



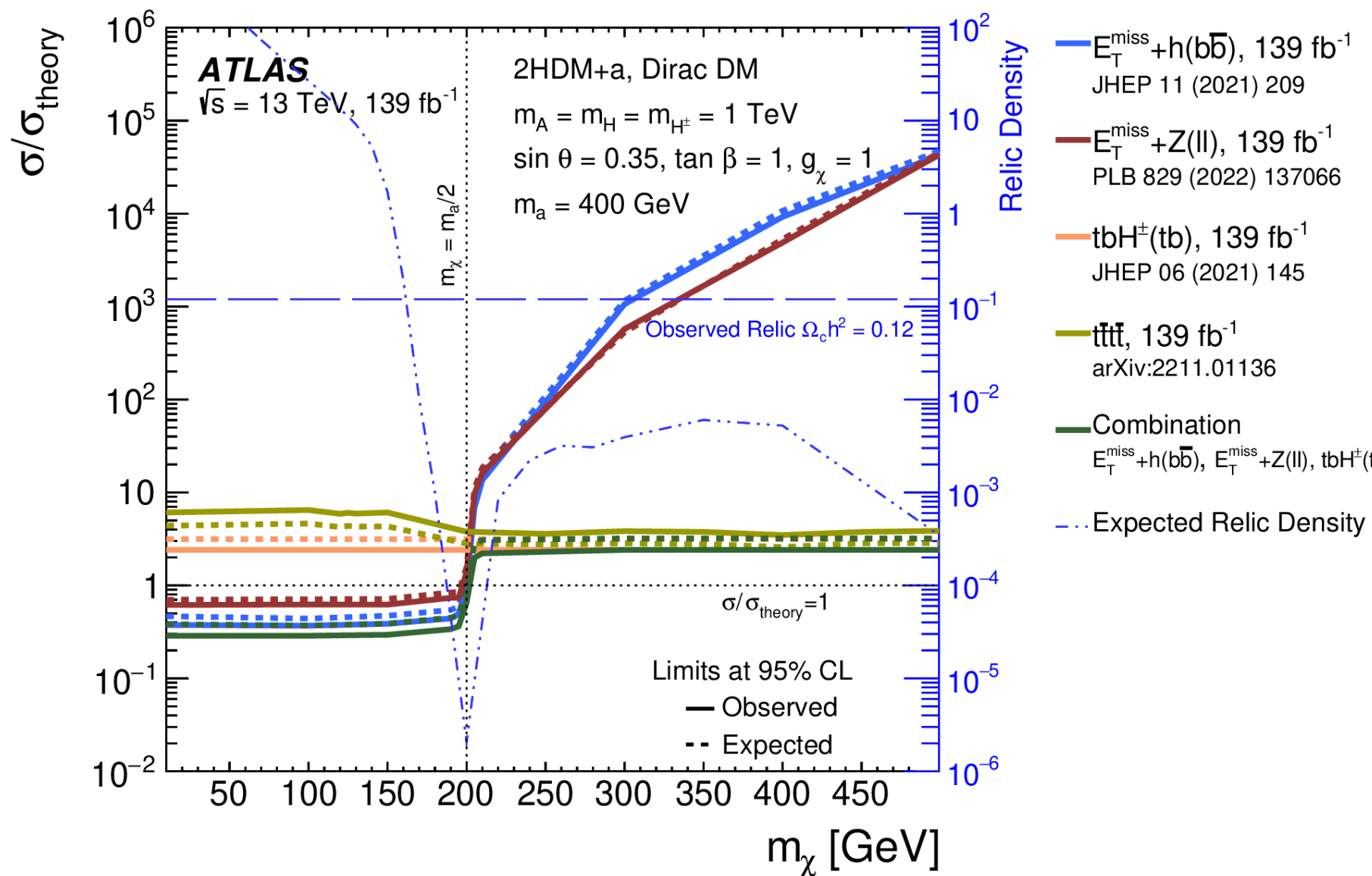
- $E_T^{miss} + h(b\bar{b})$, JHEP 11 (2021)
- $E_T^{miss} + h(\gamma\gamma)$, JHEP 10 (2021)
- $E_T^{miss} + Z(ll)$, PLB 829 (2022)
- $E_T^{miss} + Z(q\bar{q})$, JHEP 10 (2018)
- $E_T^{miss} + Wt$, arXiv:2211.1313
- $E_T^{miss} + j$, PRD 103 (2021)
- $tbH^\pm(tb)$, JHEP 06 (2021)
- Combination of $E_T^{miss} + h(b\bar{b})$



- $t\bar{t}\bar{t}$, 139 fb, arXiv:2211.0113
- $E_T^{miss} + t\bar{t}$, 36, EPJC 78 (2018)
- $E_T^{miss} + b\bar{b}$, 3, EPJC 78 (2018)

Scenario 5: m_χ scan

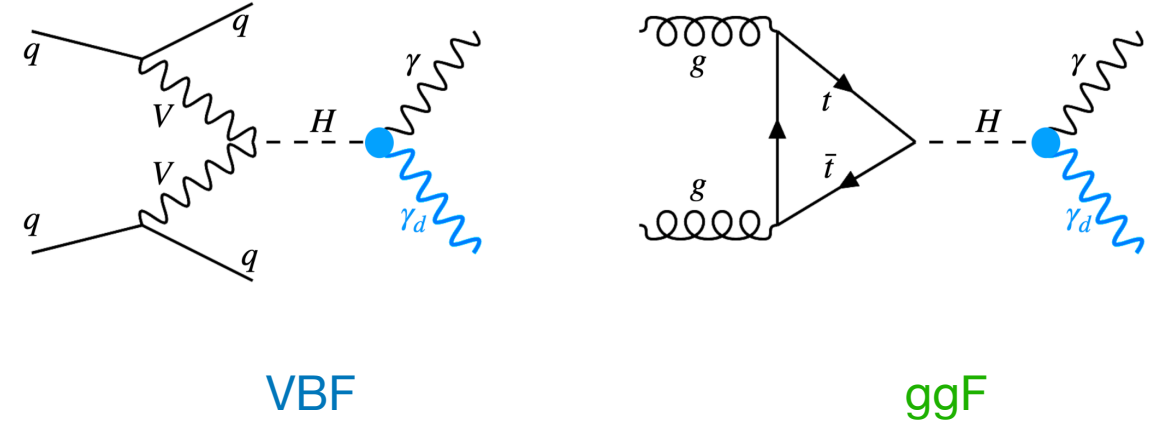
- At low- m_χ ($m_\chi < m_a/2$) sensitivity is driven by $E_T^{miss} + Z(ll)$ and $E_T^{miss} + h(bb)$ as the pseudoscalar is allowed to decay in to $\chi\chi$.
- For higher DM masses ($m_\chi > m_a/2$), the sensitivity of $E_T^{miss} + X$ decreases rapidly, while that of $tbH^\pm(tb)$ and $4top$ remains nearly constant. Although none of them excludes 2HDM+a.
- Combination provides strongest exclusion.
- Possible to match the observed relic density for $m_\chi \approx 170$ GeV without changing the collider phenomenology.



Mono-photon re-interpretation for $H \rightarrow \gamma\gamma_d$

- re-interpretation of $E_T^{\text{miss}} + \gamma$ to search for dark photon in high-mass resonances.

- $m_H \in [400, 3000]$ GeV; massless dark photon;
- dark photon $\rightarrow E_T^{\text{miss}}$.



- Include contribution from both VBF and ggF production modes.
- Discriminant variable: E_T^{miss} .

